

Morphology-dependent resonances in homogeneous and core-shell nonspherical particlesBenjamin Vennes and Thomas C. Preston ^{*}*Department of Atmospheric and Oceanic Sciences and Department of Chemistry, McGill University,
805 Sherbrooke Street West, Montreal, Quebec, Canada H3A 0B9* (Received 21 May 2021; revised 18 August 2021; accepted 23 August 2021; published 10 September 2021)

We formulate a perturbation theory for determining the frequencies of quasinormal modes in dielectric nonspherical core-shell particles. The theory is based on the extended boundary condition method (also known as the null-field method), which is used to represent the internal field in terms of a matrix Q . In this framework, the excitation of a morphology-dependent resonance corresponds to a vanishing eigenvalue of the Q matrix, which can be determined using perturbation techniques to yield explicit formulas for the corresponding eigenfrequency. We specialize our results to the case of a core-shell spherical particle that has been deformed into a spheroid and provide a comparison between numerical simulations and the perturbation theory. Excellent agreement is found for the small perturbations considered here. Further, we investigate the eigenfrequencies of core-shell particles for an extensive range of parameters.

DOI: [10.1103/PhysRevA.104.033512](https://doi.org/10.1103/PhysRevA.104.033512)**I. INTRODUCTION****A. Morphology-dependent resonances**

Dielectric microparticles can behave as high-quality factor Q optical cavities that confine the electromagnetic field to a region of space [1,2]. This confinement is not absolute and the resulting resonant states are dissipative modes of the leaky optical cavity [3]. Due to their finite lifetime, these are quasinormal modes and, in discussions of microparticles, are commonly referred to as morphology-dependent resonances (MDRs) [4,5]. In open electromagnetic resonators, the energy of a given mode leaks out of the resonator due to coupling to the external medium [6]. In microspheres, Q depends on several loss channels and optical modes can easily be spoiled by asphericity [7]. This ultimately results in a vast range of observed Q from $\sim 10^2$ to 10^9 [8,9].

Morphology-dependent resonances can be modeled as eigenfunctions of the sourceless Maxwell wave equation subject to the outgoing-wave radiation condition [10]. Given the non-Hermitian nature of the problem, the corresponding eigenfrequencies are complex, with the imaginary part being related to the rate of dissipation of the mode. The eigenfrequencies of the quasinormal modes are poles in the complex plane of the scattering matrix of the open cavity [11]. For instance, the resonance condition for a homogeneous sphere can readily be found by setting the denominators of the Mie scattering coefficients to zero [12]. For resonances in the optical spectrum of this well-studied system, the real part of the complex eigenfrequency is the peak position and the imaginary part determines the peak linewidth [13].

If an arbitrary inhomogeneity is introduced in the spherical particle or the surface of the particle is deformed, then the eigenfrequency is not as readily obtained and methods such as perturbative techniques can be employed to retrieve them.

Perturbation theories such as the resonant state expansion have been used for determining the eigenfrequencies of three-dimensional (3D) optical cavities with an arbitrary dielectric inhomogeneity [14]. Similarly, the dyadic formulation of MDRs [15] and its perturbation theory [16,17] accomplishes the same goal. For shape deformations, examples of perturbation theories include the boundary perturbation method for 2D and 3D resonators [18,19], a perturbation theory based on the Kapur-Peierls formalism [20], and a quasinormal mode perturbation theory based on the Lippmann-Schwinger equation [21].

In this paper we provide a perturbation theory for calculating the eigenfrequencies of a core-shell spherical particle with small axisymmetric deformations. The technique developed in this work differs from prior ones in two key ways. First, in our approach, a perturbation theory is applied to the Stratton-Chu equations. The use of surface integral equations to describe the electromagnetic fields is important to the proposed shape perturbation theory given that any change in the surface profile of either the core or the shell is immediately reflected in the surface integrals. Second, the subsequent application of the extended boundary condition method (EBCM) confines the problem to the interior of the resonator as boundary conditions are met when employing the EBCM. Using field expansions in spherical vector wave functions (SVWFs), the internal field coefficients are linearly related to the incident field through a Q matrix, which can be readily determined for core-shell structures. By associating a resonant state with a particular vanishing eigenvalue of the Q matrix, we employ matrix perturbation theory to find explicit formulas for the shift in the MDR eigenfrequencies. Therefore, for these two reasons, this perturbation technique is particularly well suited for core-shell particles. A complete discussion of the theory is provided in Sec. II.

The motivation for studying deformed core-shell particle systems will be outlined here. Applications of core-shell MDRs for a system composed of a sphere with a concentric

^{*}thomas.preston@mcgill.ca

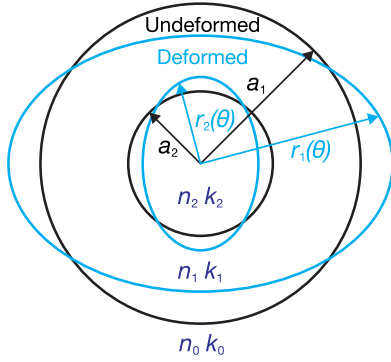


FIG. 1. Geometry of the undeformed and deformed core-shell particle.

spherical shell are numerous. The sensitivity of MDRs allows for nanometer thin coatings on micron-sized droplets to be characterized with high precision [22]. Shifts in core-shell MDRs allow for the position of sharp diffusion fronts during solvent uptake in spherical particles to be tracked [23,24]. This has found application in monitoring water uptake in high-viscosity aerosol particles in order to study condensed phase diffusion [25–27]. In the same field of atmospheric aerosol science, core-shell MDRs have now been used in many studies of liquid-liquid phase separation [28–31]. Thin coatings on microspheres can also be used to improve the sensitivity of MDR-based sensors [32,33].

For a homogeneous spherical particle, deformation leads to breaking of spherical symmetry and the loss of azimuthal degeneracy. Morphology-dependent resonance peaks then split into multiplets. This has been observed in a myriad of experiments [34–37] and can be accurately predicted using an analytic formula given by Lai *et al.* [38]. For a deformed core-shell particle, similar splitting is anticipated due to the lower symmetry, but there is currently no analogous formula. Further, the investigation of the deformation of such optical cavities is lacking. Morphology-dependent resonances could enable the detection of nanometer deformations in core-shell systems allowing, for instance, simultaneous measurement of both surface and interfacial tension of phase-separated droplets. This particle morphology and its surface tension are now recognized to be key to understanding cloud droplet activation in a variety of circumstances [39,40]. Finally, core-shell particles are known to have optical properties that cannot be realized in homogeneous spheres, e.g., with thicker shells, the excitation of core resonances can result in sharp extinction

minima [41], which makes investigations into their optical properties worthwhile in their own right.

B. Eigenfrequencies of spheroidal core-shell particles

The application of the perturbation theory to the quasi-normal modes of the core-shell system shown in Fig. 1 is discussed in Sec. II. For readers who wish to bypass that discussion, here we summarize one of the main results from our work: formulas for the first-order shifts in the eigenfrequencies (i.e., the resonant frequency of MDRs) of a spherical core-shell particle that is deformed into a spheroid. The eigenfrequencies of the core-shell particle are labeled according to their angular momentum numbers and polarization type (l, m, p) , where l is the mode number, m is the azimuthal mode number bounded by $-l \leq m \leq l$, and p denotes either transverse electric (TE) or transverse magnetic (TM) polarization.

The unperturbed core-shell particle and its physical parameters are shown in Fig. 1. The shell (core) has a radius a_1 (a_2) and refractive index n_1 (n_2). The core-shell ratio is $\alpha = a_2/a_1$. Upon being perturbed, it will be convenient to expand the shell and core deformation (r_1 and r_2 , respectively) in Legendre polynomials as

$$r_j(\theta) = a_j + \sum_{L=0}^{\infty} h_L^{(j)} P_L(\cos \theta), \quad (1)$$

where $h_L^{(j)}$ are the expansion coefficients of the deformation. For the case of interest where $L = 2$, the core and the shell are deformed into spheroids and we define the eccentricity of the core (e_c) and shell (e_s) according to

$$e_c = \frac{r_2(\theta = 0^\circ) - r_2(\theta = 90^\circ)}{a_2},$$

$$e_s = \frac{r_1(\theta = 0^\circ) - r_1(\theta = 90^\circ)}{a_1}. \quad (2)$$

With these definitions, the fractional shift of a MDR labeled (l, m, p) is found by using the formulas presented in Sec. II B, from which the equation

$$\frac{\Delta v_{lm}^p}{v_l^p} = \frac{1}{6} \frac{R_l^p \alpha e_c + e_s}{R_l^p \alpha + 1} \left(\frac{3m^2}{l(l+1)} - 1 \right), \quad (3)$$

is obtained, where Δv_{lm}^p is the first-order shift and v_l^p is the eigenfrequency of the undeformed system. We note that the magnitude of the fractional shift depends on the physical parameters of the core-shell particle. In addition, the term R_l^p also incorporates these dependences as it is a function of the undeformed core-shell particle

$$R_l^{\text{TE}} = \frac{n_2^2 - n_1^2}{n_1^2 - 1} \left[\frac{\psi_l(n_2 x_2)}{\xi_l(x_1)} \frac{\xi_l'(x_1) \psi_l(n_1 x_1) - n_1 \psi_l'(n_1 x_1) \xi_l(x_1)}{n_1 \psi_l'(n_1 x_2) \psi_l(n_2 x_2) - n_2 \psi_l'(n_2 x_2) \psi_l(n_1 x_2)} \right]^2, \quad (4)$$

$$R_l^{\text{TM}} = \frac{n_2^2 - n_1^2}{n_1^2 - 1} \frac{l(l+1) \psi_l^2(n_2 x_2)/(n_1 x_2)^2 + [\psi_l'(n_2 x_2)]^2}{l(l+1) \xi_l^2(x_1)/(n_1 x_1)^2 + [\xi_l'(x_1)]^2} \left[\frac{n_1 \xi_l'(x_1) \psi_l(n_1 x_1) - \psi_l'(n_1 x_1) \xi_l(x_1)}{n_2 \psi_l'(n_1 x_2) \psi_l(n_2 x_2) - n_1 \psi_l'(n_2 x_2) \psi_l(n_1 x_2)} \right]^2, \quad (5)$$

where $x_1 = k_0 a_1$ and $x_2 = \alpha x_1$ are the resonant size parameters of the core-shell sphere. The Ricatti-Bessel functions ψ_l and ξ_l are related to the spherical Bessel function and spherical Hankel function of the first kind as $\psi_l(x) = x j_l(x)$ and $\xi_l(x) = x h_l^{(1)}(x)$. In

order to evaluate R_l^p , it is necessary to solve for the resonant size parameter of the core-shell sphere using numerical root-finding methods, which have been discussed in detail elsewhere [42]. Finally, we note that the degeneracy of the m th azimuthal mode is lifted according to a quadratic function in m , which remains the same quadratic function as reported for the homogeneous case. Approximations to Eq. (3) can be obtained in the limit where the shell is very thin compared to the outer radius. These formulas are convenient since the dependence on the resonant core-shell size parameter is removed, thus alleviating the need for any numerical methods that the general solution requires. In addition, they still remain functions of the refractive indices of the core and the thin shell. Insofar as the shell surface and core-shell interface do not touch, the thin shell limit simplifies the fractional shift to

$$\frac{\Delta v_{lm}^{\text{TE}}}{v_l^{\text{TE}}} = \frac{1}{6} \frac{(n_2^2 - n_1^2)e_c + (n_1^2 - 1)e_s}{n_2^2 - 1} \left(\frac{3m^2}{l(l+1)} - 1 \right), \quad (6)$$

$$\frac{\Delta v_{lm}^{\text{TM}}}{v_l^{\text{TM}}} = \frac{1}{6} \frac{(n_2^2 - n_1^2)[1 + n_1^2(n_2^2 - 1)]e_c + (n_1^2 - 1)[n_2^2 + n_1^2(n_2^2 - 1)]e_s}{n_1^2 n_2^2 (n_2^2 - 1)} \left(\frac{3m^2}{l(l+1)} - 1 \right), \quad (7)$$

where the TM formula is accurate up to $O(l^{-2/3})$ since we have made use of the fact that the homogeneous size parameter is $n_2 x \sim l[1 + O(l^{-2/3})]$. The fractional shift in the eigenfrequencies given by Eq. (3) and the thin shell limit of Eqs. (6) and (7) are the main results of this work. The following section elaborates on the formalism used to derive it.

II. RESONANCE CONDITION UNDER SHAPE PERTURBATIONS

In the T -matrix formalism, the electromagnetic fields incident on and scattered by an arbitrarily shaped particle are expanded in SVWFs with a time-harmonic dependence $\exp(-i\omega t)$. Then, the expansion coefficients of the internal and scattered fields, denoted by \mathbf{a}_{int} and \mathbf{a}_{sca} , are linearly related to the incident field \mathbf{a}_{inc} through the Q and T matrices as

$$Q\mathbf{a}_{\text{int}} = \mathbf{a}_{\text{inc}}, \quad \mathbf{a}_{\text{sca}} = P\mathbf{a}_{\text{int}}, \quad \mathbf{a}_{\text{sca}} = T\mathbf{a}_{\text{inc}} = PQ^{-1}\mathbf{a}_{\text{inc}}, \quad (8)$$

where we write the T matrix as the product of two matrices P and Q^{-1} in anticipation of the use of the EBCM. Consider the first of these equations in the absence of a source field \mathbf{a}_{inc} ; then the homogeneous equation $Q\mathbf{a}_{\text{int}} = 0$ has two possible solutions: (i) the trivial solution where the coefficients vanish, which is of no interest, and (ii) the internal field is in a resonant state given by the equation $\det(Q) = 0$. One can search for the zeros of the determinant numerically as was done in Ref. [43] Alternatively, for the second solution, we can define a resonant state when one of the eigenvalues of Q , denoted by λ_{lm}^p , is set to zero. Although straightforward in concept, an analytic expression for λ_{lm}^p is difficult and even impossible to find unless some assumptions are made concerning the geometry of the particle. Here we will assume that the deviation from spherical symmetry is small enough so that we can employ matrix perturbation theory to find explicit formulas for the eigenvalues to first order. In turn, fulfilling the resonant condition $\lambda_{lm}^p = 0$ will yield the formula for the fractional shift in the eigenfrequency.

Now we will present the main result for first-order perturbation theory to the eigenvalues of the matrix. Beforehand, we remark that Q is a non-Hermitian matrix (i.e., has complex eigenvalues), so special care has to be taken when using per-

turbation theory. This is typically addressed by exploiting the biorthogonality of the eigenvectors of the matrix of interest with its adjoint eigenvectors [44]. However, given that the initial matrix that will be perturbed is diagonal, this means that the initial eigenvectors are already orthogonal. So the results from perturbation theory for Hermitian matrices are immediately carried over. Therefore, for an axisymmetric deformation where $Q \rightarrow Q^{(0)} + \epsilon Q^{(1)}$, the new eigenvalues are changed to first order according to

$$\lambda_{lm}^p = Q_{lm}^{p(0)} + \epsilon Q_{lm}^{p(1)}, \quad (9)$$

where $Q_{lm}^{p(0)}$ denotes the diagonal element of the zeroth-order Q matrix and $Q_{lm}^{p(1)}$ is the first-order diagonal element of the perturbation Q matrix. Note that when we set $\lambda_{lm}^p = 0$ in Eq. (9), ϵ is used to mark terms of different orders, meaning that each term will be individually zero.

Expressions for the Q matrix are needed to proceed further and these are given by using the EBCM. A brief review of this method is as follows: Fictitious surface currents coincide with the surface of the particle to produce the internal and external fields that would arise through the scattering process. For the time being, we can assume the particle is homogeneous so that, on its external surface denoted by S_1 and regardless of the existence of internal layers, the fields are given by [45]

$$\begin{aligned} \mathbf{E}_{\text{inc}}(\mathbf{r}) + \nabla \times \int_{S_1} [\mathbf{n}_1 \times \mathbf{E}_1(\mathbf{r}_S)] \cdot \vec{G}(k_0 R) dS \\ - \frac{Z_0}{ik_0} \nabla \times \nabla \times \int_{S_1} [\mathbf{n}_1 \times \mathbf{H}_1(\mathbf{r}_S)] \cdot \vec{G}(k_0 R) dS \\ = \begin{cases} \mathbf{E}_{\text{sca}}(\mathbf{r}) + \mathbf{E}_{\text{inc}}(\mathbf{r}) & \text{if } \mathbf{r} \text{ lies outside } S_1 \\ \mathbf{0} & \text{if } \mathbf{r} \text{ lies inside } S_1, \end{cases} \end{aligned} \quad (10)$$

where k_0 is the wave number and Z_0 is the impedance in the surrounding medium. The electric fields \mathbf{E}_{inc} , \mathbf{E}_{sca} , and \mathbf{E}_1 are the incident, scattered, and internal fields, respectively (\mathbf{H}_1 is the internal magnetic field). Finally, the Green's dyadic in free space is $\vec{G}(k_0 R)$, with $R = |\mathbf{r} - \mathbf{r}_S|$. For a homogeneous particle, this equation alone is sufficient to solve for the Q matrix by assuming SVWF expansions for the Green's dyadic

and the internal field (see, e.g., Ref. [45]) to give

$$\mathcal{Q}_{\text{hom}} = [\mathcal{Q}_1^{31}] = \begin{bmatrix} [K_1^{31}] + \eta_1 [J_1^{31}] & [L_1^{31}] + \eta_1 [I_1^{31}] \\ [I_1^{31}] + \eta_1 [L_1^{31}] & [J_1^{31}] + \eta_1 [K_1^{31}] \end{bmatrix}, \quad (11)$$

where $\eta_1 = Z_0/Z_1$ and I, J, K, L are block matrices. In anticipation of the core-shell system, it is convenient to introduce generalized definitions of this matrix and its blocks in Eq. (11). For the i th interface, we introduce

$$[\mathcal{Q}_i^{jk}] = \begin{bmatrix} [K_i^{jk}] + \eta_i [J_i^{jk}] & [L_i^{jk}] + \eta_i [I_i^{jk}] \\ [I_i^{jk}] + \eta_i [L_i^{jk}] & [J_i^{jk}] + \eta_i [K_i^{jk}] \end{bmatrix}, \quad (12)$$

for which the elements of the block matrices are given by the surface integrals

$$[I_i^{jk}]_{ll'mm'} = k_{i-1}^2 \int_{S_i} \mathbf{n}_i \cdot [\mathbf{M}_{lm}^{(j)*}(k_{i-1}\mathbf{r}_S) \times \mathbf{M}_{l'm'}^{(k)}(k_i\mathbf{r}_S)] dS, \quad (13)$$

$$[J_i^{jk}]_{ll'mm'} = k_{i-1}^2 \int_{S_i} \mathbf{n}_i \cdot [\mathbf{M}_{lm}^{(j)*}(k_{i-1}\mathbf{r}_S) \times \mathbf{N}_{l'm'}^{(k)}(k_i\mathbf{r}_S)] dS, \quad (14)$$

$$[K_i^{jk}]_{ll'mm'} = k_{i-1}^2 \int_{S_i} \mathbf{n}_i \cdot [\mathbf{N}_{lm}^{(j)*}(k_{i-1}\mathbf{r}_S) \times \mathbf{M}_{l'm'}^{(k)}(k_i\mathbf{r}_S)] dS, \quad (15)$$

$$[L_i^{jk}]_{ll'mm'} = k_{i-1}^2 \int_{S_i} \mathbf{n}_i \cdot [\mathbf{N}_{lm}^{(j)*}(k_{i-1}\mathbf{r}_S) \times \mathbf{N}_{l'm'}^{(k)}(k_i\mathbf{r}_S)] dS, \quad (16)$$

where it should be clear that j and k denote the radial wave functions used in the SVWF expansion. Note that square brackets were employed in Eqs. (11)–(16) to distinguish the indices (i, j, k) from the elements (or entries) of the matrices.

If the particle is a core-shell one, then an additional surface equation is needed to account for scattering between the shell and the core [46],

$$\begin{aligned} & \nabla \times \int_{S_1} [-\mathbf{n}_1 \times \mathbf{E}_1(\mathbf{r}_S)] \cdot \vec{G}(k_1 R) dS \\ & - \frac{Z_1}{ik_1} \nabla \times \nabla \times \int_{S_1} [-\mathbf{n}_1 \times \mathbf{H}_1(\mathbf{r}_S)] \cdot \vec{G}(k_1 R) dS \\ & + \nabla \times \int_{S_2} [\mathbf{n}_2 \times \mathbf{E}_2(\mathbf{r}_S)] \cdot \vec{G}(k_1 R) dS \\ & - \frac{Z_1}{ik_1} \nabla \times \nabla \times \int_{S_2} [\mathbf{n}_2 \times \mathbf{H}_2(\mathbf{r}_S)] \cdot \vec{G}(k_1 R) dS \\ & = \begin{cases} \mathbf{E}_1(\mathbf{r}) & \text{if } \mathbf{r} \text{ lies between } S_2 \text{ and } S_1 \\ \mathbf{0} & \text{if } \mathbf{r} \text{ lies inside } S_2 \text{ or outside } S_1, \end{cases} \end{aligned} \quad (17)$$

where now \mathbf{E}_1 and \mathbf{H}_1 denote the electric and magnetic fields in the shell, \mathbf{E}_2 and \mathbf{H}_2 denote the electric and magnetic fields in the core, S_2 denotes the core surface, and k_2 is the wave number in the core. In the case of the core-shell system, the procedure is similar to the homogeneous case and the \mathcal{Q} matrix found is

$$\mathcal{Q}_{\text{core-shell}} = [\mathcal{Q}_1^{31}][\mathcal{Q}_2^{31}] - [\mathcal{Q}_1^{33}][\mathcal{Q}_2^{11}]. \quad (18)$$

In the following sections, we will present the procedure to extract the frequency shift from both homogeneous and

core-shell particles with an axisymmetric deformation. The homogeneous case serves the dual purpose of (i) illustrating the method without excessive algebra and (ii) validating the method based on already existing results. Thereafter, we will summarize the procedure to extract the shifts in the eigenfrequencies for core-shell particles based on the method presented for the homogeneous case.

A. Homogeneous axisymmetric particle

We will start by considering the TE case, for which the elements $\mathcal{Q}_{lm}^{p(0)}$ and $\mathcal{Q}_{lm}^{p(1)}$ are found from the diagonal elements of the first block matrix of Eq. (11). For an axisymmetric scatterer, these surface integrals are reduced to line integrals in the polar angle as

$$\mathcal{Q}_{lm}^{\text{TE}} = \int_0^\pi \sin \theta d\theta |\mathbf{X}_{lm}|^2 W_1^{31}(x_1), \quad (19)$$

where $x_1 = k_0 r_1(\theta)$ is a size parameter that depends on the variation of the surface profile r_1 and on the wave number k_0 , and $W_1^{31}(x_1)$ is a radial function defined as

$$W_1^{31}(x_1) = \xi_l'(x_1) \psi_l(n_1 x_1) - n_1 \psi_l'(n_1 x_1) \xi_l(x_1). \quad (20)$$

Although it is only a minor point, a coefficient $-1/n_1$ was omitted in the definition of $W_1^{31}(x_1)$ as it factors out in the analysis. In the limit where the deviation from spherical geometry is small, we can expand both the wave number k_0 and the radial profile $r_1(\theta)$ in terms of a power series characterized by a small parameter ($\epsilon \ll 1$)

$$r_1(\theta) = r^{(0)} + \epsilon r^{(1)}(\theta) = a_1 + \epsilon \sum_L h_L P_L(\cos \theta), \quad (21)$$

$$k_0 = k^{(0)} + \epsilon k^{(1)} + O(\epsilon^2), \quad (22)$$

where $r^{(0)} = a_1$ corresponds to the radius of the unperturbed spherical particle and $r^{(1)}(\theta)$ is the deviation from the spherical geometry written in terms of an arbitrary superposition of Legendre polynomials. In turn, $k^{(0)}$ is the resonant wave number of the unperturbed system and $k^{(1)}$ is the first-order correction due to the distortion. It is convenient to combine both expansions in terms of the size parameter

$$\begin{aligned} x_1 &= x_1^{(0)} + \epsilon x_1^{(1)} + O(\epsilon^2) \\ &= k^{(0)} r^{(0)} + \epsilon (k^{(0)} r^{(1)} + k^{(1)} r^{(0)}) + O(\epsilon^2), \end{aligned} \quad (23)$$

because the Taylor expansion of the radial function $W_1^{31}(x_1)$ can be written as

$$W_1^{31}(x_1) = W_1^{31}(x_1^{(0)}) + \epsilon x_1^{(1)} [W_1^{31}(x_1^{(0)})]'. \quad (24)$$

With the use of the expansion of $W(x_1)$ given by Eq. (24), we may write down the zeroth- and first-order elements of the \mathcal{Q} matrix in Eq. (9) and set each term to zero as

$$\mathcal{Q}_{lm}^{\text{TE}(0)} = W_1^{31}(x_1^{(0)}) \int_0^\pi \sin \theta d\theta |\mathbf{X}_{lm}|^2 = 0, \quad (25)$$

$$\mathcal{Q}_{lm}^{\text{TE}(1)} = [W_1^{31}(x_1^{(0)})]' \int_0^\pi \sin \theta d\theta |\mathbf{X}_{lm}|^2 x_1^{(1)} = 0. \quad (26)$$

The zeroth-order equation leads to the well-known TE resonance condition of spherical dielectric particles. The angular

integral is nonzero and so the equation is satisfied when $W_1^{31}(x_1^{(0)}) = 0$, for which

$$\xi_l'(x_1^{(0)})\psi_l(n_1x_1^{(0)}) - n_1\psi_l'(n_1x_1^{(0)})\xi_l(x_1^{(0)}) = 0, \quad (27)$$

where $x_1^{(0)}$ is the resonant size parameter and so, as was already discussed, $k^{(0)}$ is the resonant wave number of the unperturbed system. Now, from the first-order equation, we seek to determine the first-order correction $k^{(1)}$. Substituting $x^{(1)}$ in terms of k and r , we have

$$[W_1^{31}(x_1^{(0)})]' \int_0^\pi \sin\theta d\theta |\mathbf{X}_{lm}|^2 (k^{(0)}r^{(1)} + k^{(1)}r^{(0)}) = 0. \quad (28)$$

When solving for the first-order correction, we recall that $r^{(1)} = \sum_L h_L P_L$, where h_L is an arbitrary coefficient and P_L is the Legendre polynomial. Therefore, by using this expansion and various properties of the Legendre polynomial, we determine $k^{(1)}$ as the summation over the coefficients h_L ,

$$\frac{k^{(1)}}{k^{(0)}} = \sum_L \left(\frac{-h_L}{a_1} \right) \left[1 - \frac{L(L+1)}{2l(l+1)} \right] \frac{\langle P_l^m | P_L | P_l^m \rangle}{\langle P_l^m | P_l^m \rangle}, \quad (29)$$

where the polar integrals are

$$\begin{aligned} \langle P_l^m | P_L | P_l^m \rangle &= \int_0^\pi \sin\theta d\theta P_l^m P_L P_l^m, \\ \langle P_l^m | P_l^m \rangle &= \int_0^\pi \sin\theta d\theta P_l^m P_l^m. \end{aligned} \quad (30)$$

The solution to the former integral can be expressed using the 3- j symbols

$$\begin{aligned} \langle P_l^m | P_L | P_l^m \rangle &= (-1)^m (2l+1) \sqrt{L + \frac{1}{2}} \\ &\times \begin{pmatrix} l & l & L \\ 0 & 0 & 0 \end{pmatrix} \begin{pmatrix} l & l & L \\ m & -m & 0 \end{pmatrix}, \end{aligned} \quad (31)$$

while the solution to the latter integral is simply given by the orthogonality of the Legendre polynomial

$$\langle P_l^m | P_l^m \rangle = 1. \quad (32)$$

Therefore, an analytic formula for the first-order shift in the eigenfrequency of a TE mode is

$$\begin{aligned} \frac{k^{(1)}}{k^{(0)}} &= (-1)^{m+1} (2l+1) \sum_L \left(\frac{h_L}{a_1} \right) \sqrt{L + \frac{1}{2}} \left[1 - \frac{L(L+1)}{2l(l+1)} \right] \\ &\times \begin{pmatrix} l & l & L \\ 0 & 0 & 0 \end{pmatrix} \begin{pmatrix} l & l & L \\ m & -m & 0 \end{pmatrix}, \end{aligned} \quad (33)$$

which is in perfect agreement with the result given by Lai *et al.* up to an additional factor of $\sqrt{2}$ absent in this work. This discrepancy is simply the result of the difference in the normalization of the Legendre polynomial.

Next, for the TM mode, the line integral that needs to be considered is from the fourth block matrix in Eq. (11),

$$Q_{lm}^{\text{TM}} = \int_0^\pi \sin\theta d\theta \left[|\mathbf{X}_{lm}|^2 X_1^{31}(x_1) + P_l^m \frac{dP_l^m}{d\theta} \frac{dx_1}{d\theta} Y_1^{31}(x_1) \right], \quad (34)$$

where we have defined the two radial functions $X_1^{31}(x_1)$ and $Y_1^{31}(x_1)$ as

$$X_1^{31}(x_1) = n_1 \xi_l'(x_1) \psi_l(n_1 x_1) - \psi_l'(n_1 x_1) \xi_l(x_1), \quad (35)$$

$$Y_1^{31}(x_1) = (n_1^2 - 1) l(l+1) \frac{\xi_l(x_1) \psi_l(n_1 x_1)}{n_1 x_1^2}. \quad (36)$$

These radial functions are also expanded in powers of ϵ in a process similar to that outlined in Eqs. (21)–(24). However, it is not necessary to expand Y_1^{31} in a Taylor series due to the fact that the derivative in θ of the surface profile $r_1(\theta)$ is assumed to scale with ϵ ,

$$\frac{dx_1}{d\theta} = \epsilon k^{(0)} \frac{dr^{(1)}(\theta)}{d\theta} + O(\epsilon^2) = \epsilon \frac{dx_1^{(1)}}{d\theta} + O(\epsilon^2), \quad (37)$$

where we have used $r_1(\theta) = r^{(0)} + r^{(1)}(\theta)$. Now conducting the same analysis as before, we find that the zeroth-order wave number satisfies the resonant condition for TM modes and its first-order correction is given by

$$\begin{aligned} \frac{k^{(1)}}{k^{(0)}} &= (-1)^{m+1} (2l+1) \sum_L \left(\frac{h_L}{a_1} \right) \\ &\times \sqrt{L + \frac{1}{2}} \left[1 - A_l(x_1^{(0)}) \frac{L(L+1)}{2l(l+1)} \right] \\ &\times \begin{pmatrix} l & l & L \\ 0 & 0 & 0 \end{pmatrix} \begin{pmatrix} l & l & L \\ m & -m & 0 \end{pmatrix}, \end{aligned} \quad (38)$$

with $A_l(x_1^{(0)})$ to be evaluated at the TM resonant size parameter of the sphere

$$A_l(x) = \left[1 + \frac{l(l+1)}{x^2} \left(\frac{\psi_l(n_1 x)}{\psi_l'(n_1 x)} \right)^2 \right]^{-1}. \quad (39)$$

This differs from the solution given by Lai *et al.* in that an additional factor of A_l has been introduced. In general, A_l is complex, which means that the TM quality factor can be changed to first order. However, in the limit where the deformation mode number L is much smaller than the resonant mode number l under consideration (i.e., $L^2/l^2 \ll 1$), this difference between the TE and TM cases is small and can be neglected. We note that in the work of Lai *et al.*, the $O(L^2/l^2)$ contribution due to A_l was dropped. We will do the same to simplify our expression to match their result

$$\begin{aligned} \frac{k^{(1)}}{k^{(0)}} &= (-1)^{m+1} (2l+1) \sum_L \left(\frac{h_L}{a_1} \right) \sqrt{L + \frac{1}{2}} \left[1 - \frac{L(L+1)}{2l(l+1)} \right] \\ &\times \begin{pmatrix} l & l & L \\ 0 & 0 & 0 \end{pmatrix} \begin{pmatrix} l & l & L \\ m & -m & 0 \end{pmatrix}, \end{aligned} \quad (40)$$

which is accurate up to $O(L^2/l^2)$.

B. Core-shell axisymmetric particle

In the core-shell case, we recall that the overall Q matrix was a product of individual Q matrices evaluated at the core-shell interface as

$$Q_{\text{core-shell}} = [Q_1^{31}][Q_2^{31}] - [Q_1^{33}][Q_2^{11}] = AB - CD, \quad (41)$$

where the matrices A , B , C , and D are identical to $[Q_1^{31}]$, $[Q_2^{31}]$, $[Q_1^{33}]$, and $[Q_2^{11}]$, respectively, and are introduced here

for brevity. To proceed, each term in Eq. (41) is expanded to first order, which will give an equation in the form of

$$\lambda_{lm}^p = [A_{lm}^{p(0)} B_{lm}^{p(0)} - C_{lm}^{p(0)} D_{lm}^{p(0)}] + \epsilon [A_{lm}^{p(0)} B_{lm}^{p(1)} + A_{lm}^{p(1)} B_{lm}^{p(0)} - C_{lm}^{p(0)} D_{lm}^{p(1)} - C_{lm}^{p(1)} D_{lm}^{p(0)}] + O(\epsilon^2), \quad (42)$$

with the higher-order terms omitted. Therefore, all that is needed now is the first-order Taylor expansion of the terms A – D . This is shown in Appendix A.

Using Eqs. (A5)–(A8), the zeroth-order term leads to the requirement that the zeroth-order wave number $k^{(0)}$ satisfies the resonance condition of the unperturbed core-shell particle

for TE modes

$$\frac{n_1 \psi_l'(n_1 x_2^{(0)}) \psi_l(n_2 x_2^{(0)}) - n_2 \psi_l(n_1 x_2^{(0)}) \psi_l'(n_2 x_2^{(0)})}{n_1 \xi_l'(n_1 x_2^{(0)}) \psi_l(n_2 x_2^{(0)}) - n_2 \xi_l(n_1 x_2^{(0)}) \psi_l'(n_2 x_2^{(0)})} = \frac{\xi_l'(x_1^{(0)}) \psi_l(n_1 x_1^{(0)}) - n_1 \xi_l(x_1^{(0)}) \psi_l'(n_1 x_1^{(0)})}{\xi_l'(x_1^{(0)}) \xi_l(n_1 x_1^{(0)}) - n_1 \xi_l(x_1^{(0)}) \xi_l'(n_1 x_1^{(0)})}. \quad (43)$$

Next, the second term will yield an equation which can be solved for the first-order correction $k^{(1)}$. It is only an algebraic exercise to extract the first-order correction using Eqs. (A5)–(A12), the result of which is

$$\frac{k^{(1)}}{k^{(0)}} = - \sum_L \frac{R_l^{\text{TE}} h_L^{(2)} + h_L^{(1)}}{R_l^{\text{TE}} a_2 + a_1} \left[1 - \frac{L(L+1)}{2l(l+1)} \right] \frac{\langle P_l^m | P_L | P_l^m \rangle}{\langle P_l^m | P_l^m \rangle}, \quad (44)$$

where R_l^{TE} is a function that depends on the physical parameters of the undeformed core shell

$$R_l^{\text{TE}} = \frac{W_1^{33}(x_1^{(0)}) [W_2^{11}(x_2^{(0)})]' - W_1^{31}(x_1^{(0)}) [W_2^{31}(x_2^{(0)})]'}{W_2^{11}(x_2^{(0)}) [W_1^{33}(x_1^{(0)})]' - W_2^{31}(x_2^{(0)}) [W_1^{31}(x_1^{(0)})]'}. \quad (45)$$

To simplify this equation to that given in Sec. IB, we first make use of the resonance condition of the unperturbed core-shell particle to find that

$$R_l^{\text{TE}} = \left(\frac{W_1^{31}(x_1^{(0)})}{W_2^{11}(x_2^{(0)})} \right)^2 \frac{W_2^{31}(x_2^{(0)}) [W_2^{11}(x_2^{(0)})]' - W_2^{11}(x_2^{(0)}) [W_2^{31}(x_2^{(0)})]'}{W_1^{31}(x_1^{(0)}) [W_1^{33}(x_1^{(0)})]' - W_1^{33}(x_1^{(0)}) [W_1^{31}(x_1^{(0)})]'}. \quad (46)$$

Next, by using the definition of W_i^{jk} and the Wronskian of the Ricatti-Bessel functions

$$\xi_l'(x) \psi_l(x) - \psi_l'(x) \xi_l(x) = i, \quad (47)$$

we find the expression that was given in the earlier summary

$$R_l^{\text{TE}} = \frac{n_2^2 - n_1^2}{n_1^2 - 1} \left[\frac{\psi_l(n_2 x_2^{(0)})}{\xi_l(x_1^{(0)})} \frac{\xi_l'(x_1^{(0)}) \psi_l(n_1 x_1^{(0)}) - n_1 \psi_l'(n_1 x_1^{(0)}) \xi_l(x_1^{(0)})}{n_1 \psi_l'(n_1 x_2^{(0)}) \psi_l(n_2 x_2^{(0)}) - n_2 \psi_l'(n_2 x_2^{(0)}) \psi_l(n_1 x_2^{(0)})} \right]^2. \quad (48)$$

For the TM case, the resonance condition of the unperturbed system is given by using the zeroth-order equations (A17)–(A20) to yield

$$\frac{n_2 \psi_l'(n_1 x_2^{(0)}) \psi_l(n_2 x_2^{(0)}) - n_1 \psi_l(n_1 x_2^{(0)}) \psi_l'(n_2 x_2^{(0)})}{n_2 \xi_l'(n_1 x_2^{(0)}) \psi_l(n_2 x_2^{(0)}) - n_1 \xi_l(n_1 x_2^{(0)}) \psi_l'(n_2 x_2^{(0)})} = \frac{n_1 \xi_l'(x_1^{(0)}) \psi_l(n_1 x_1^{(0)}) - \xi_l(x_1^{(0)}) \psi_l'(n_1 x_1^{(0)})}{n_1 \xi_l'(x_1^{(0)}) \xi_l(n_1 x_1^{(0)}) - \xi_l(x_1^{(0)}) \xi_l'(n_1 x_1^{(0)})}. \quad (49)$$

For the first-order correction, we use Eqs. (A17)–(A24) to find that the fractional shift can be expressed as

$$\frac{k^{(1)}}{k^{(0)}} = - \sum_L \frac{R_l^{\text{TM}} h_L^{(2)}}{R_l^{\text{TM}} a_2 + a_1} \left[1 - A_l(x_2^{(0)}) \frac{L(L+1)}{2l(l+1)} \right] \frac{\langle P_l^m | P_L | P_l^m \rangle}{\langle P_l^m | P_l^m \rangle} - \sum_L \frac{h_L^{(1)}}{R_l^{\text{TM}} a_2 + a_1} \left[1 - B_l(x_1^{(0)}) \frac{L(L+1)}{2l(l+1)} \right] \frac{\langle P_l^m | P_L | P_l^m \rangle}{\langle P_l^m | P_l^m \rangle}, \quad (50)$$

where the zeroth-order wave number must satisfy the resonance condition for TM modes. Notice that, similar to the homogeneous case, we have the added complexity of two functions A_l and B_l introduced in the ratio of the total mode numbers. If we perform the same approximation as given by Lai *et al.*, we may readily drop those terms and get a formula accurate up to $O(L^2/l^2)$. The full derivation of A_l and B_l as well as that of R_l^{TM} is given in Appendix B. Briefly, the procedure is essentially the same as in the TE case: We use the resonance condition and the Wronskian of the Ricatti-Bessel function to derive simpler expressions than what is initially found,

$$R_l^{\text{TM}} = \frac{n_2^2 - n_1^2}{n_1^2 - 1} \left[\frac{B_l(x_2^{(0)})}{A_l(x_1^{(0)})} \left(\frac{\psi_l'(n_2 x_2^{(0)})}{\xi_l'(x_1^{(0)})} \frac{n_1 \xi_l'(x_1^{(0)}) \psi_l(n_1 x_1^{(0)}) - \psi_l'(n_1 x_1^{(0)}) \xi_l(x_1^{(0)})}{n_2 \psi_l'(n_1 x_2^{(0)}) \psi_l(n_2 x_2^{(0)}) - n_1 \psi_l'(n_2 x_2^{(0)}) \psi_l(n_1 x_2^{(0)})} \right)^2 \right], \quad (51)$$

while A_l and B_l are

$$A_l(x) = \left[1 + \frac{l(l+1)}{(n_1 x)^2} \left(\frac{\psi_l(n_2 x)}{\psi_l'(n_2 x)} \right)^2 \right]^{-1}, \quad (52)$$

$$B_l(x) = \left[1 + \frac{l(l+1)}{(n_1 x)^2} \left(\frac{\xi_l(x)}{\xi_l'(x)} \right)^2 \right]^{-1}. \quad (53)$$

This effectively concludes the determination of the fractional shift in the eigenfrequencies of a core-shell particle perturbed by an arbitrary axisymmetric deformation. The fractional shifts for TE and TM modes are given by Eqs. (44) and (50), respectively. However, the solution that we found, even though it is in closed form, is rather cumbersome. Determining the fractional shift requires the evaluation of the 3- j symbol as well as radial functions which depend on the resonant size parameter of the core-shell particle [Eq. (48) for TE modes and Eqs. (51)–(53) for TM modes]. Ultimately, the most imposing task is the determination of the TE and TM resonant size parameters which are the roots of the transcendental equations given by Eqs. (43) and (49), respectively. In the following, we specialize our result in order to find simpler formulas. We will describe the case of a core-shell particle that has been deformed into a spheroid as well as its limiting case of a very thin shell.

To describe the spheroid, we use a quadrupole perturbation $L = 2$ and we assume that the mode number of the MDR has $l \gg L$. With this, the angular integral (31) is

$$\langle P_l^m | P_2 | P_l^m \rangle = \sqrt{\frac{5}{2}} \frac{l(l+1) - 3m^2}{(2l-1)(2l+3)} \approx \sqrt{\frac{5}{32}} \left(1 - \frac{3m^2}{l(l+1)} \right), \quad (54)$$

and using the definition of the Legendre polynomials, we define the amplitude of deformation e as

$$e = 3\sqrt{\frac{5}{8}} \frac{h}{a}. \quad (55)$$

With these two results, the solution reduces to Eq. (3), which was given in Sec. IB. Further, in the limit of a thin shell, we may approximate the core-shell particle by setting $x_2^{(0)} \rightarrow x_1^{(0)}$. In this limit, R_l^{TE} and R_l^{TM} are approximated as

$$R_l^{\text{TE}} \approx \frac{n_2^2 - n_1^2}{n_1^2 - 1}, \quad (56)$$

$$R_l^{\text{TM}} \approx \frac{n_2^2 - n_1^2}{n_1^2 - 1} \frac{1 + n_1^2(n_2^2 - 1)}{n_2^2 + n_1^2(n_2^2 - 1)}, \quad (57)$$

which are used to give Eqs. (6) and (7).

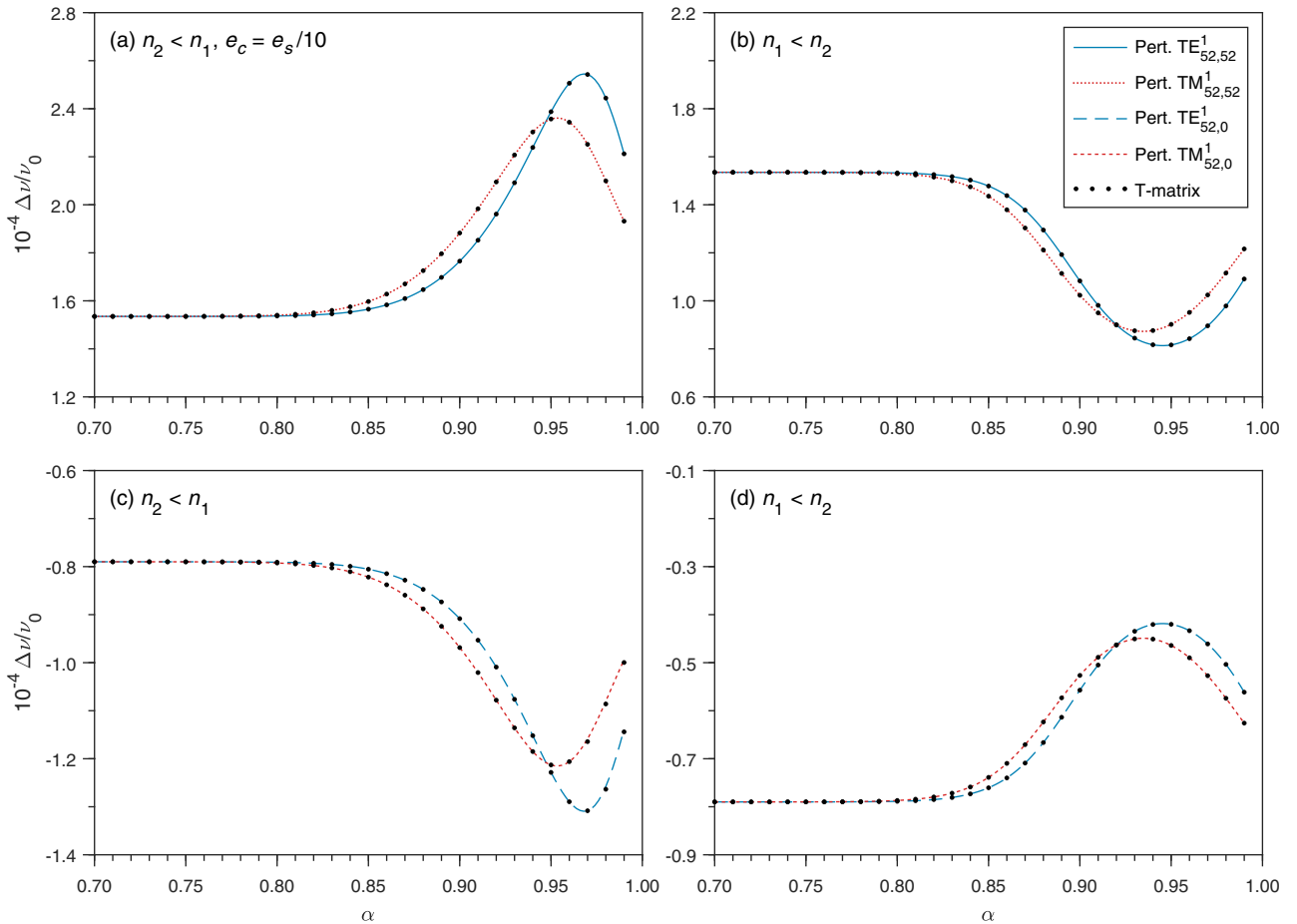


FIG. 2. Fractional shift of the $\text{TE}_{52,m}^1$ and $\text{TM}_{52,m}^1$ modes for $m = 0$ and 52 as a function of the core-shell ratio α . In all four panels, the shell (core) is deformed into a prolate spheroid with $e_s = 4.743 \times 10^{-4}$ ($e_c = e_s/10$). In (a) and (c) the shell (core) has a refractive index of $n_1 = 1.41$ ($n_2 = 1.33$) and in (b) and (d) these values are exchanged.

III. RESULTS AND DISCUSSION

In this discussion, we assess the accuracy of the first-order perturbation theory by comparing it to a full numerical implementation of the T -matrix formalism. In the framework of the EBCM, the T matrix of a core-shell particle is the solution to Eqs. (10) and (17) for the scattered field coefficients [46]

$$T_1 = \{[Q_1^{11}] - [Q_1^{13}]T_2\} \{[Q_1^{31}] - [Q_1^{33}]T_2\}^{-1}, \quad (58)$$

where $T_2 = [Q_2^{11}][Q_2^{31}]^{-1}$ is the T matrix of the core embedded in a medium comprised of the shell. The orientation-averaged extinction efficiency is given by the trace of the real part of the T matrix [47]

$$\langle Q_{\text{ext}} \rangle = \frac{2}{x^2} \sum_{l=1}^{\infty} \sum_{m=0}^l (2 - \delta_{m,0}) \text{Re}(T_{l1mm}^{11} + T_{l1mm}^{22}). \quad (59)$$

By calculating Eq. (59) at a specified value of m across a range of wavelengths, we associate a maximum in $\langle Q_{\text{ext}} \rangle$ with a particular MDR. Note: $\langle Q_{\text{ext}} \rangle$ should not be confused with the Q matrix.

In Fig. 2 we compare the fractional shift given by perturbation theory with the full numerical calculation using the T matrix. Excellent agreement is found between the two calculations. In Figs. 2(a)–2(d) the shell and the core are both prolate spheroids as they are characterized by a quadrupole distortion with $e_s = 4.743 \times 10^{-4}$ and $e_c = 4.743 \times 10^{-5}$, respectively. In Figs. 2(a) and 2(b) the fractional shifts of the $\text{TE}_{52,52}^1$ and $\text{TM}_{52,52}^1$ are positive and shows that the $m = l$ modes blueshift with respect to the unperturbed case. However, the magnitude of the shift depends on the core-shell ratio and the relative refractive index between the core and the shell. In Fig. 2(a), when $n_1 < n_2$, a maximum is attained at $\alpha \sim 0.97$ ($\alpha \sim 0.95$) for TE (TM) modes. In contrast, when $n_2 < n_1$ in Fig. 2(b), a minimum is reached at $\alpha \sim 0.95$ ($\alpha \sim 0.93$) for TE (TM) modes. In both Figs. 2(a) and 2(b), when the shell reaches a thickness of $\alpha < 0.8$, the fractional shift becomes insensitive to the core-shell ratio and to the refractive indices. In this thick shell limit, the fractional shift corresponds to that of a homogeneous dielectric particle perturbed by the shell quadrupole distortion. For a homogeneous particle, the first-order shift is independent of the characteristics of the unperturbed particle and is given by

$$\frac{\Delta v_{lm}^p}{v_l^p} = \frac{e}{6} \left(\frac{3m^2}{l(l+1)} - 1 \right), \quad (60)$$

which is why the thick shell limit gives the same fractional shift in both Figs. 2(a) and 2(b). In Figs. 2(c) and 2(d), where $m = 0$, the fractional shift is negative and so the modes redshift with respect to the unperturbed case. Apart from this change in sign, the preceding remarks concerning the magnitude of the shift are carried over. This is a consequence of the fact that the first-order solution decouples the quadratic function in the azimuthal mode m from the other terms.

The resulting pattern is made clear once we plot $\langle Q_{\text{ext}} \rangle$ as a function of wavelength. This is shown in Fig. 3, where in Fig. 3(a) we choose the value of α that coincides with the maximum possible splitting as inferred from Figs. 2(a) and 2(c). We compare this to the ‘‘homogeneous equivalent’’ system, which is the homogeneous particle where the unperturbed

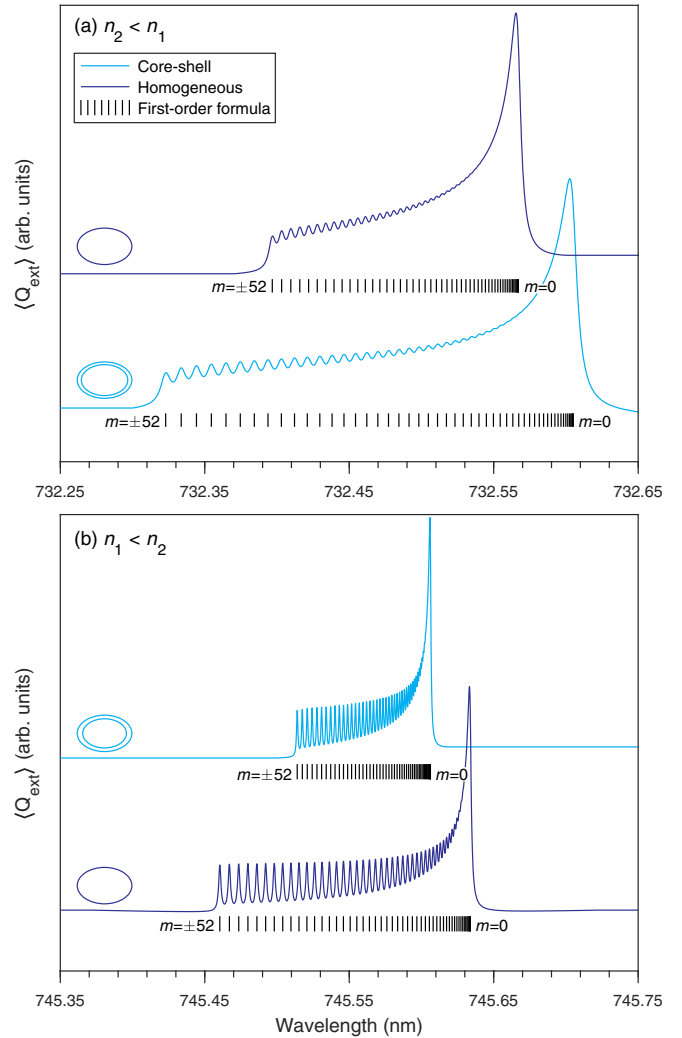


FIG. 3. Orientation-averaged extinction cross section of the $\text{TE}_{52,m}^1$ modes as a function of the wavelength. The core-shell ratio is set to (a) $\alpha = 0.97$ and (b) $\alpha = 0.95$. Otherwise, the physical parameters are identical to those listed in Fig. 2. The homogeneous equivalent system has a refractive index of (a) $n_{\text{hom}} = 1.354$ ($n_2 < n_1$) and (b) $n_{\text{hom}} = 1.379$ ($n_1 < n_2$).

MDR frequency coincides with that of the unperturbed core-shell system. This homogeneous particle is characterized by the shell quadrupole distortion. Clearly, the core-shell particle with $n_2 < n_1$ has an increase in splitting when compared to the homogeneous case. In contrast, in Fig. 3(b) the value of α coincides with the minimal splitting in Figs. 3(a) and 3(c). Here the core-shell particle with $n_1 < n_2$ has a decrease in the splitting with respect to the homogeneous case.

The resonant size parameter of the unperturbed core-shell particle that satisfies Eq. (43) or (49) has an infinite number of roots, which is referred to as the mode order. Physically, the order of a MDR is associated with the number of radial maxima in the angular averaged energy density of the mode in question [48]. In the previous figures we used first-order MDRs (i.e., the first root). Figure 4 shows the case of second-order MDRs, namely, the $\text{TE}_{52,m}^2$ and $\text{TM}_{52,m}^2$ modes. Essentially, there is a clear variation in α of the splitting as it undulates between an increase (a decrease) and no increase

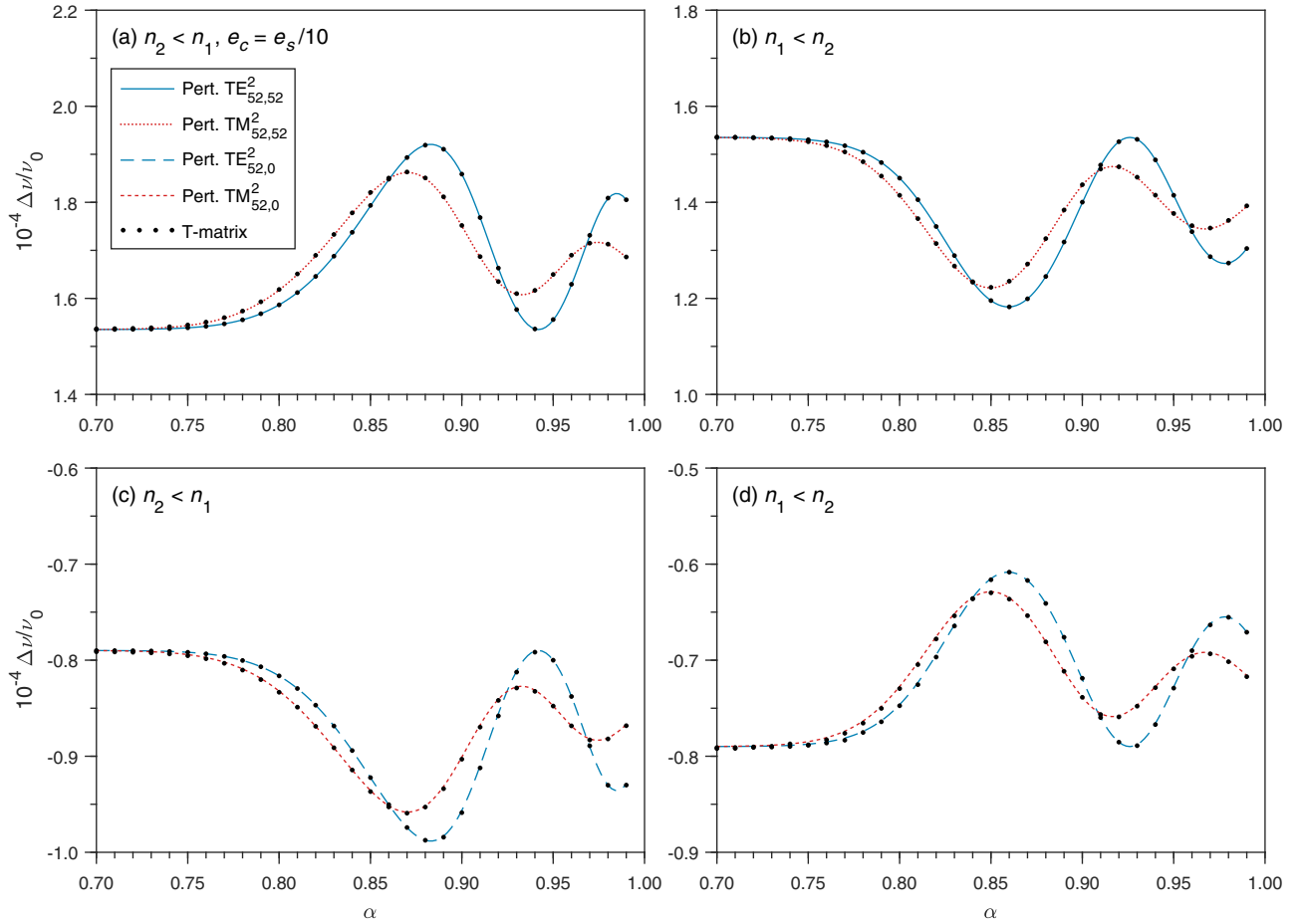


FIG. 4. Fractional shift of the $\text{TE}_{52,m}^2$ and $\text{TM}_{52,m}^2$ modes for $m = 0$ and 52 as a function of the core-shell ratio α . In all four panels, the shell (core) is deformed into a prolate spheroid with $e_s = 4.743 \times 10^{-4}$ ($e_c = e_s/10$). In (a) and (c) the shell (core) has a refractive index of $n_1 = 1.5$ ($n_2 = 1.45$) and in (b) and (d) these values are exchanged.

(decrease) with respect to the thick shell limit. For first-order modes as in Fig. 2, we have one maximum (minimum) in α , whereas for second-order modes, we have two maxima (minima) in α . So, in contrast to the homogeneous case, there is an implicit dependence of the fractional shift on the order of the mode. This dependence is evident once we consider that the fractional shift is a function of the resonant size parameter, which in turn must be a root of Eq. (43) or (49).

In Fig. 5 the fractional shift as a function of α is shown for a range of azimuthal modes from $m = 0$ to $m = l$ in increments of 4. The parameters chosen correspond to those in Figs. 2(a) and 2(b), respectively. So the features that were discussed are already apparent here. For a selected range of the core-shell ratio in Fig. 5(a), there is an increase in the splitting with respect to the homogeneous system, whereas in Fig. 5(b) there is a decrease in the splitting. In Figs. 5(c) and 5(d) the values of the quadrupole distortions are exchanged (i.e., the core is more eccentric than the shell), which results in a very particular behavior. Specifically, in Fig. 5(c) we observe that as the shell gets thinner (increasing α), all the modes converge onto zero at $\alpha^* \sim 0.89$ (0.88) for TE (TM) modes. In effect, despite the fact that the core-shell particle is nonspherical, no splitting occurs for this particular combination of physical parameters. After this point, the pattern is essentially inverted

and the modes that were redshifted before now blueshift and vice versa. This is a special case where a core-shell prolate spheroid can give rise to the same behavior as a homogeneous oblate spheroid, in which the $m = l$ modes redshift. This behavior is made clear once we consider the numerator of Eq. (3),

$$N = R_l^p \alpha e_c + e_s. \quad (61)$$

The condition of no splitting in the modes is fulfilled trivially when the particle is spherical ($e_c = e_s = 0$). However, we can also have no splitting, at least to first order, provided the eccentricity of the core and shell are related by

$$e_c = -\frac{e_s}{R_l^p \alpha}, \quad (62)$$

which is precisely what occurs at the nodes $\alpha = \alpha^*$ in Fig. 5(c). When $\alpha < \alpha^*$, the modes behave as we would expect because $N > 0$, and when $\alpha > \alpha^*$ the behavior inverts as $N < 0$.

In Fig. 6 we show the fractional shift when the core is oblate (i.e., negative eccentricity) with all other parameters carried over from Fig. 5. In Figs. 6(a) and 6(b) the features that were seen in Figs. 5(a) and 5(b) are apparent here. However, the difference is that the negative core eccentricity tends to

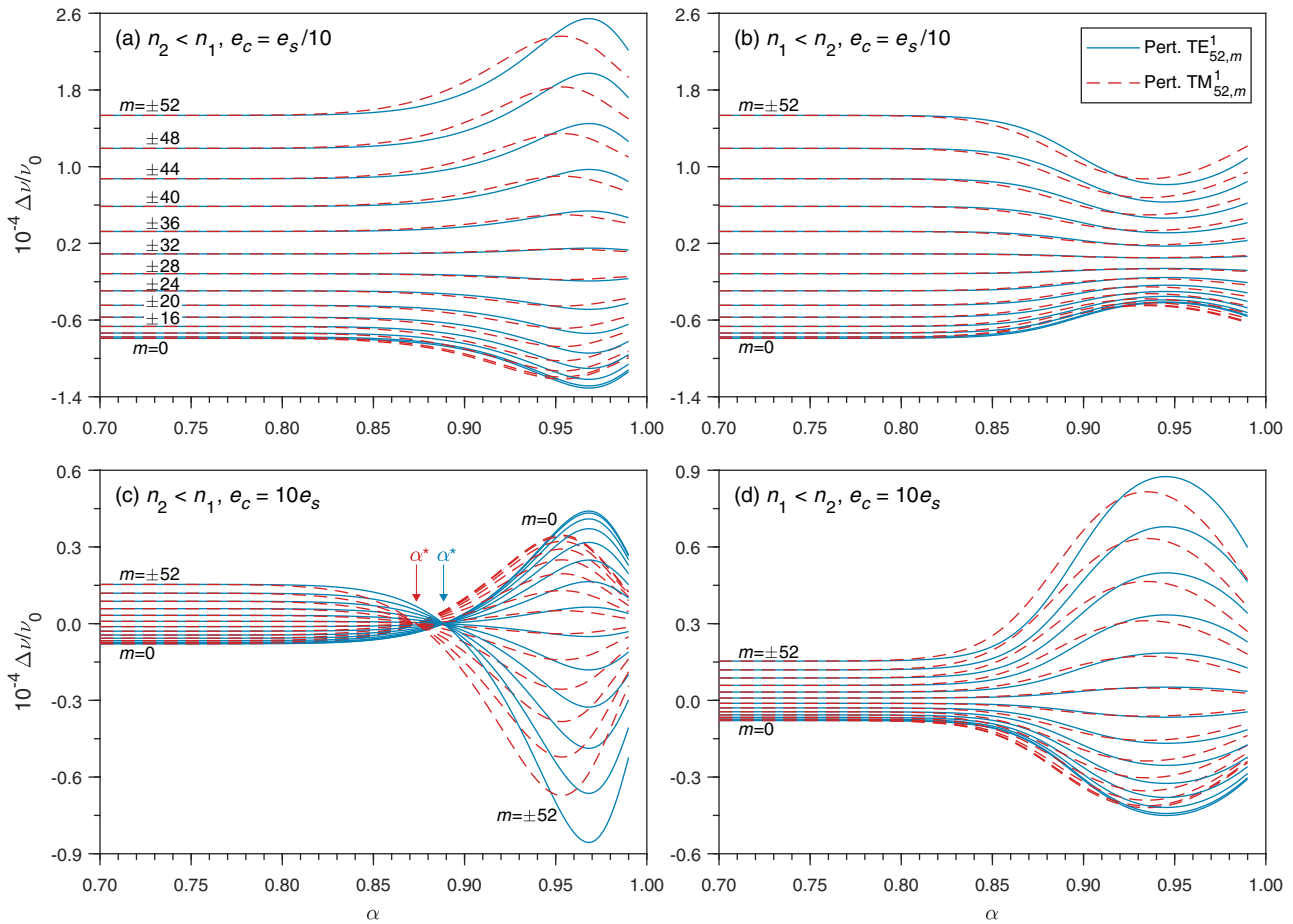


FIG. 5. Fractional shift of the $\text{TE}_{52,m}^1$ and $\text{TM}_{52,m}^1$ modes as a function of the core-shell ratio α . The shell (core) is deformed into a prolate spheroid with (a) and (b) $e_s = 4.743 \times 10^{-4}$ ($e_c = e_s/10$) and (c) and (d) $e_s = 4.743 \times 10^{-5}$ ($e_c = 10e_s$). In (a) and (c) the shell (core) has a refractive index of $n_1 = 1.41$ ($n_2 = 1.33$) and in (b) and (d) these values are exchanged.

enhance the splitting in Fig. 6(a), whereas in Fig. 6(b) it suppresses the splitting. It is noteworthy that in Figs. 6(c) and 6(d) it is now the latter that exhibits the no splitting behavior. This is a result of the change in sign of e_c , which means that the condition given in Eq. (62) can only be satisfied by an additional change in sign when $n_1 < n_2$.

In Fig. 7 the fractional shift is shown as a function of the core eccentricity in Figs. 7(a) and 7(c) and as a function of the shell eccentricity in Figs. 7(b) and 7(d) while the other is held fixed at zero. In all but one case, the pattern observed is that the $m \sim \pm l$ modes tend to blueshift (redshift) with increasing prolateness (oblateness), whereas the $m \sim 0$ modes tend to redshift (blueshift) with increasing prolateness (oblateness). The exception is Fig. 7(a), where $n_2 < n_1$ and $e_s = 0$. Here the pattern is flipped, as the $m \sim \pm l$ modes tend to redshift (blueshift) with increasing prolateness (oblateness) and vice versa for the $m \sim 0$ modes. So a prolate (oblate) core embedded in a spherical coating with a smaller refractive index effectively behaves as a homogeneous oblate (prolate) spheroid. In all other cases, i.e., Figs. 7(b)–7(d), the core-shell particle behaves the same as the homogeneous particle. However, we recall that for core-shell particles, the slope of

the fractional shift also depends on the polarization type of the mode, which is not the case for homogeneous particles.

In Fig. 8 we vary the core and shell eccentricities with $e_c = -e_s$. The main result of interest here is in Fig. 8(c), where the splittings of the TE modes and TM modes behave differently from one another. In effect, when the $\text{TE}_{52,\pm 52}^1$ mode redshifts, the $\text{TM}_{52,\pm 52}^1$ mode blueshifts and vice versa. This is a special case where Eq. (61) changes sign depending on the polarization type under consideration. We show this explicitly in Fig. 9, where the fractional shift is plotted as a function of core-shell ratio using the parameters from Fig. 8(c). Here the TE mode has two nodes at $\alpha^* \sim 0.93$ and another at $\alpha^* \sim 0.96$, whereas the TM mode has none. In between these two nodes, e.g., $r \sim 0.95$, the TE and TM modes split in opposite directions, as we discussed for Fig. 8(c).

Finally, although not shown here, there is another special case where the core-shell particle will behave like a homogeneous particle irrespective of the refractive indices and core-shell ratio. This occurs when the eccentricities are equal ($e_c = e_s = e$), for which the core-shell formula (3) behaves similarly to that of a homogeneous particle [Eq. (60)].

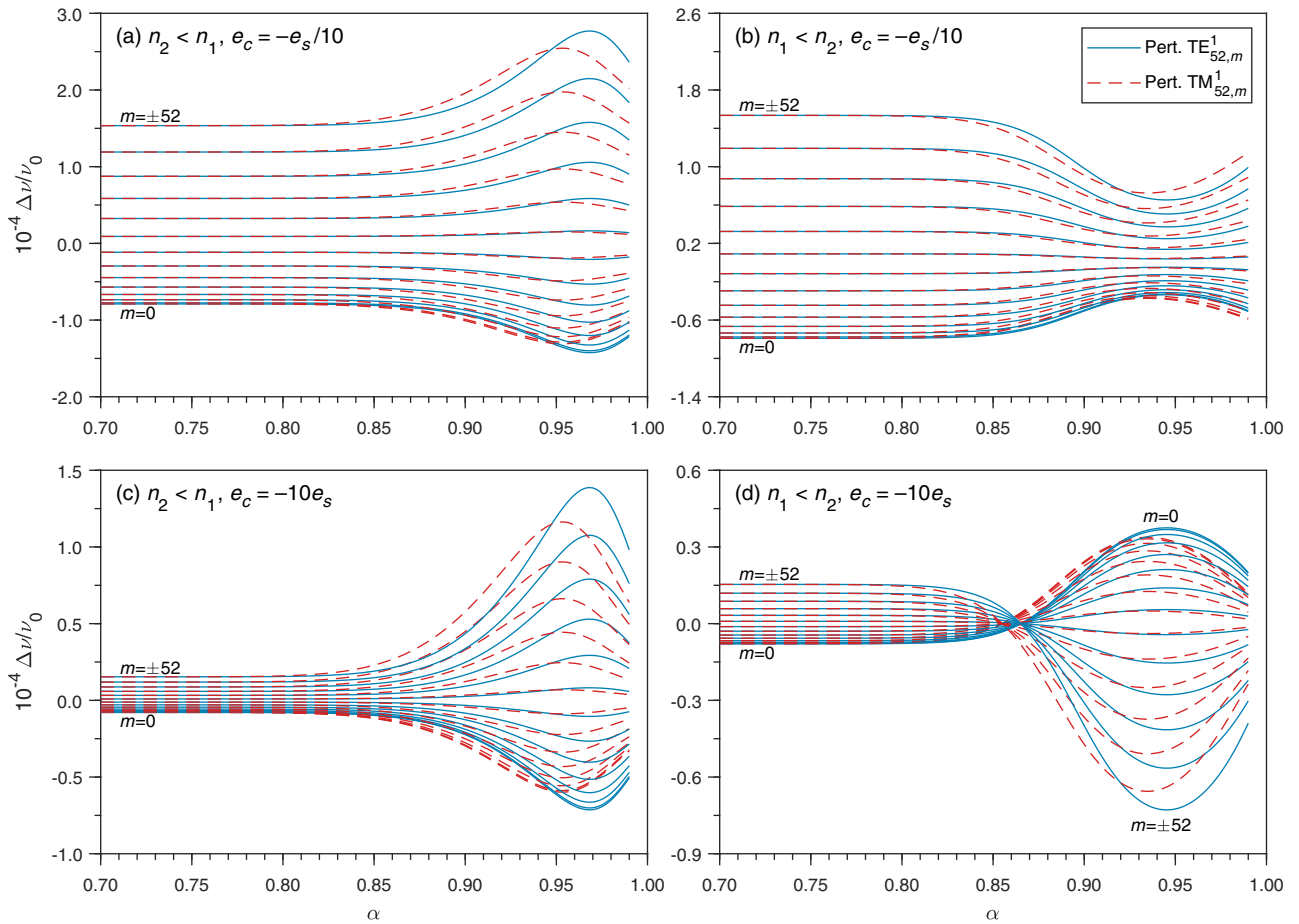


FIG. 6. Fractional shift of the $\text{TE}_{52,m}^1$ and $\text{TM}_{52,m}^1$ modes as a function of the core-shell ratio α . The shell (core) is deformed into a prolate (oblate) spheroid with (a) and (b) $e_s = 4.743 \times 10^{-4}$ ($e_c = -e_s/10$) and (c) and (d) $e_s = 4.743 \times 10^{-5}$ ($e_c = -10e_s$). In (a) and (c) the shell (core) has a refractive index of $n_1 = 1.41$ ($n_2 = 1.33$) and in (b) and (d) these values are exchanged.

IV. SUMMARY

We have presented a framework for extracting the eigenfrequencies of nonspherical core-shell particles provided the nonspherical distortion is small. The method is based on the observation that in the EBCM, a resonant state can be defined as the nontrivial solution to the equation $\mathbf{Qa}_{\text{int}} = 0$. We associate with a particular resonant state a vanishing eigenvalue $\lambda_{lm}^p = 0$. Then we employ matrix perturbation theory about a base state for which the eigenvalue is known (i.e., a radially stratified sphere) to approximate the eigenvalue of the nonspherical particle. For a core-shell particle, fulfilling the condition $\lambda_{lm}^p = 0$ allows us to extract closed-form expressions for the first-order frequency shift due to an axisymmetric deformation. In order to use the formulas, the resonant size parameter of the core-shell spherical particle needs to be known *a priori*, which requires numerical root-finding methods (however, these are well established [42] and straightforward to implement). Notwithstanding, we provide a comparison between the perturbation theory and a numerical implementation of the T -matrix method in the framework of the EBCM. For the small perturbations considered here, excellent agreement is found between the two of them. Throughout this work, we highlighted some very peculiar behavior in the

fractional shift of a MDR that can arise due to the core-shell morphology of the deformed particle. For instance, we considered the case of a prolate shell with an embedded prolate core with a smaller eccentricity. Depending on whether the core or the shell has the highest refractive index, we observe either a decrease or an increase in the splitting of the modes with respect to a homogeneous particle consisting solely of the shell. Further, we discussed the interesting case where the splitting in a core-shell particle consisting of two concentric prolate spheroids with $n_2 < n_1$ can give rise to the same splitting as in a homogeneous oblate spheroid. Finally, while we applied our formalism to core-shell particles consisting of two concentric spheroids, the perturbation theory can readily be used to determine MDR positions for other geometries. To accomplish this, one would choose a different radial profile for the particle surface.

ACKNOWLEDGMENT

T.C.P. acknowledges support from the Natural Sciences and Engineering Research Council of Canada (NSERC).

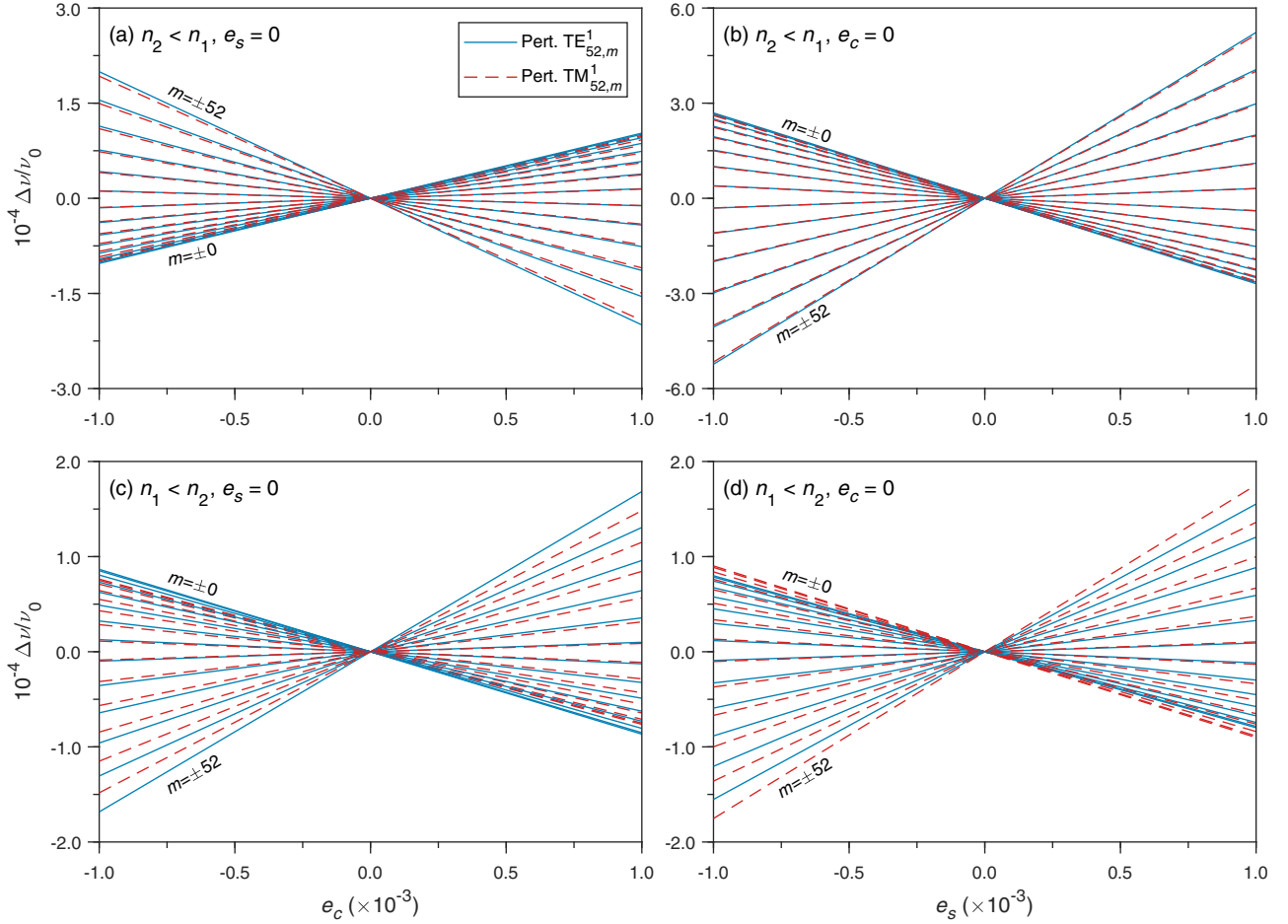


FIG. 7. Fractional shift of the $\text{TE}_{52,m}^1$ and $\text{TM}_{52,m}^1$ modes as a function of the eccentricity. (a) and (c) The core is deformed while the shell remains spherical. (b) and (d) The shell is deformed while the core remains spherical. In (a) and (b) the shell (core) has a refractive index of $n_1 = 1.41$ ($n_2 = 1.33$) and in (c) and (d) these values are exchanged. The core-shell ratio is held fixed at $\alpha = 0.95$.

APPENDIX A: LIST OF EXPRESSIONS FOR THE CORE-SHELL Q MATRICES

1. TE modes

For the core-shell system, the diagonal elements of the Q matrix for the TE mode are given by

$$A_{lm}^{\text{TE}} = \int_0^\pi \sin \theta d\theta |\mathbf{X}_{lm}|^2 W_1^{31}(x_1), \quad (\text{A1})$$

$$B_{lm}^{\text{TE}} = \int_0^\pi \sin \theta d\theta |\mathbf{X}_{lm}|^2 W_2^{31}(x_2), \quad (\text{A2})$$

$$C_{lm}^{\text{TE}} = \int_0^\pi \sin \theta d\theta |\mathbf{X}_{lm}|^2 W_1^{33}(x_1), \quad (\text{A3})$$

$$D_{lm}^{\text{TE}} = \int_0^\pi \sin \theta d\theta |\mathbf{X}_{lm}|^2 W_2^{11}(x_2). \quad (\text{A4})$$

Then the zeroth- and first-order terms in the Taylor expansions are

$$A_{lm}^{\text{TE}(0)} = W_1^{31}(x_1^{(0)}) \int_0^\pi \sin \theta d\theta |\mathbf{X}_{lm}|^2, \quad (\text{A5})$$

$$B_{lm}^{\text{TE}(0)} = W_2^{31}(x_2^{(0)}) \int_0^\pi \sin \theta d\theta |\mathbf{X}_{lm}|^2, \quad (\text{A6})$$

$$C_{lm}^{\text{TE}(0)} = W_1^{33}(x_1^{(0)}) \int_0^\pi \sin \theta d\theta |\mathbf{X}_{lm}|^2, \quad (\text{A7})$$

$$D_{lm}^{\text{TE}(0)} = W_2^{11}(x_2^{(0)}) \int_0^\pi \sin \theta d\theta |\mathbf{X}_{lm}|^2, \quad (\text{A8})$$

$$A_{lm}^{\text{TE}(1)} = [W_1^{31}(x_1^{(0)})]' \int_0^\pi \sin \theta d\theta |\mathbf{X}_{lm}|^2 x_1^{(1)}, \quad (\text{A9})$$

$$B_{lm}^{\text{TE}(1)} = [W_2^{31}(x_2^{(0)})]' \int_0^\pi \sin \theta d\theta |\mathbf{X}_{lm}|^2 x_2^{(1)}, \quad (\text{A10})$$

$$C_{lm}^{\text{TE}(1)} = [W_1^{33}(x_1^{(0)})]' \int_0^\pi \sin \theta d\theta |\mathbf{X}_{lm}|^2 x_1^{(1)}, \quad (\text{A11})$$

$$D_{lm}^{\text{TE}(1)} = [W_2^{11}(x_2^{(0)})]' \int_0^\pi \sin \theta d\theta |\mathbf{X}_{lm}|^2 x_2^{(1)}. \quad (\text{A12})$$

Similar to the homogeneous case, coefficients of $-1/n_i$ are omitted in the definitions of W_i^{jk} as they factor out in the analysis.

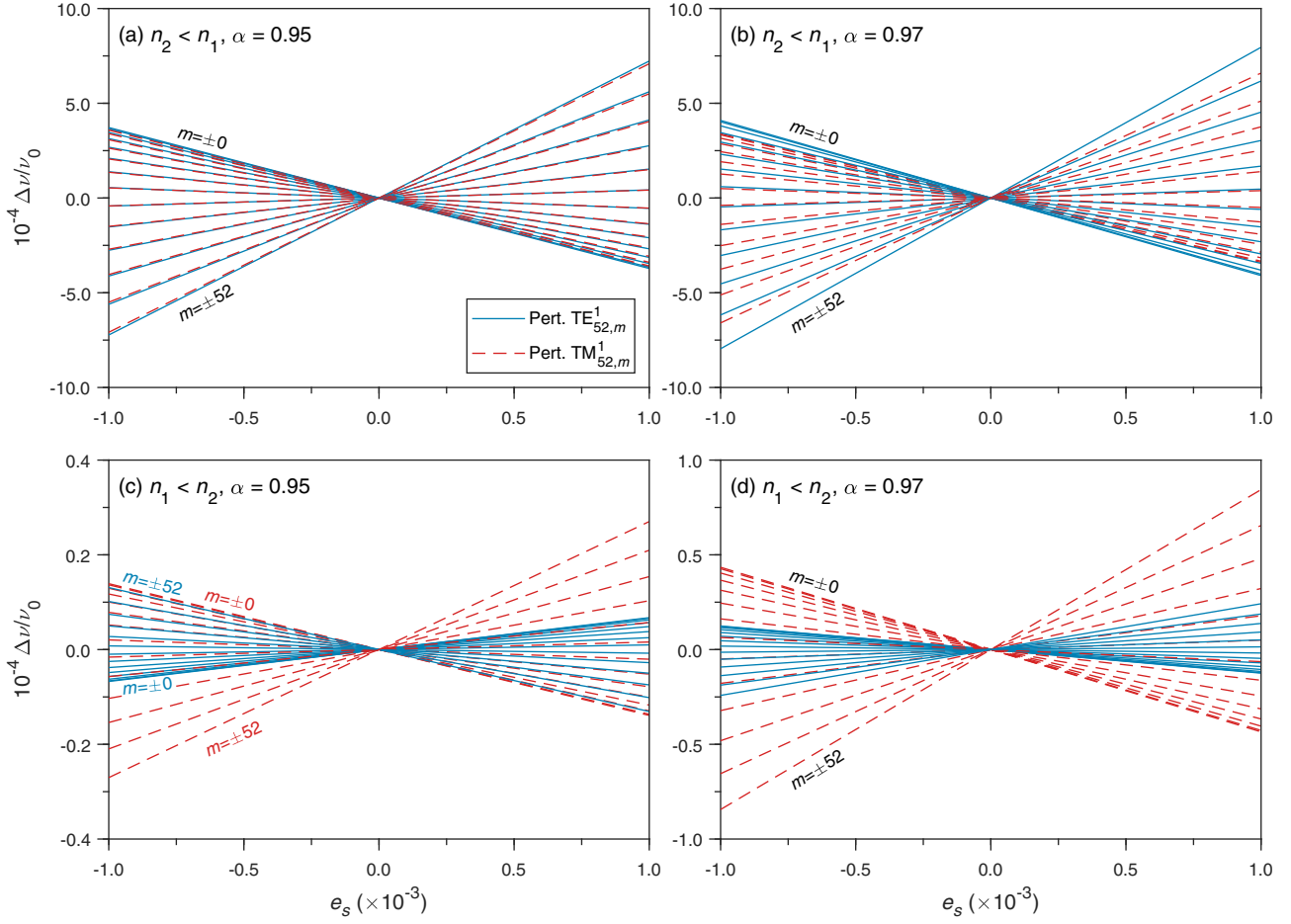


FIG. 8. Fractional shift of the $\text{TE}_{52,m}^1$ and $\text{TM}_{52,m}^1$ modes as a function of the eccentricity. In all instances, the core and shell eccentricities are related by $e_c = -e_s$. In (a) and (b) the shell (core) has a refractive index of $n_1 = 1.41$ ($n_2 = 1.33$) and in (c) and (d) these values are exchanged.

2. TM modes

Here we list the Taylor expansions necessary to conduct the analysis for TM modes:

$$A_{lm}^{\text{TM}} = \int_0^\pi \sin \theta d\theta \left[|\mathbf{X}_{lm}|^2 X_1^{31}(x_1) + P_l^m \frac{dP_l^m}{d\theta} Y_1^{31}(x_1) \right], \quad (\text{A13})$$

$$B_{lm}^{\text{TM}} = \int_0^\pi \sin \theta d\theta \left[|\mathbf{X}_{lm}|^2 X_2^{31}(x_2) + P_l^m \frac{dP_l^m}{d\theta} Y_2^{31}(x_2) \right], \quad (\text{A14})$$

$$C_{lm}^{\text{TM}} = \int_0^\pi \sin \theta d\theta \left[|\mathbf{X}_{lm}|^2 X_1^{33}(x_1) + P_l^m \frac{dP_l^m}{d\theta} Y_1^{33}(x_1) \right], \quad (\text{A15})$$

$$D_{lm}^{\text{TM}} = \int_0^\pi \sin \theta d\theta \left[|\mathbf{X}_{lm}|^2 X_2^{11}(x_2) + P_l^m \frac{dP_l^m}{d\theta} Y_2^{11}(x_2) \right], \quad (\text{A16})$$

$$A_{lm}^{\text{TM}(0)} = X_1^{31}(x_1^{(0)}) \int_0^\pi \sin \theta d\theta |\mathbf{X}_{lm}|^2, \quad (\text{A17})$$

$$B_{lm}^{\text{TM}(0)} = X_2^{31}(x_2^{(0)}) \int_0^\pi \sin \theta d\theta |\mathbf{X}_{lm}|^2, \quad (\text{A18})$$

$$C_{lm}^{\text{TM}(0)} = X_1^{33}(x_1^{(0)}) \int_0^\pi \sin \theta d\theta |\mathbf{X}_{lm}|^2, \quad (\text{A19})$$

$$D_{lm}^{\text{TM}(0)} = X_2^{11}(x_2^{(0)}) \int_0^\pi \sin \theta d\theta |\mathbf{X}_{lm}|^2, \quad (\text{A20})$$

$$A_{lm}^{\text{TM}(1)} = \int_0^\pi \sin \theta d\theta \left[|\mathbf{X}_{lm}|^2 [X_1^{31}(x_1^{(0)})]' x_1^{(1)} + P_l^m \frac{dP_l^m}{d\theta} \frac{dx_1^{(1)}}{d\theta} Y_1^{31}(x_1^{(0)}) \right], \quad (\text{A21})$$

$$B_{lm}^{\text{TM}(1)} = \int_0^\pi \sin \theta d\theta \left[|\mathbf{X}_{lm}|^2 [X_2^{31}(x_2^{(0)})]' x_2^{(1)} + P_l^m \frac{dP_l^m}{d\theta} \frac{dx_2^{(1)}}{d\theta} Y_2^{31}(x_2^{(0)}) \right], \quad (\text{A22})$$

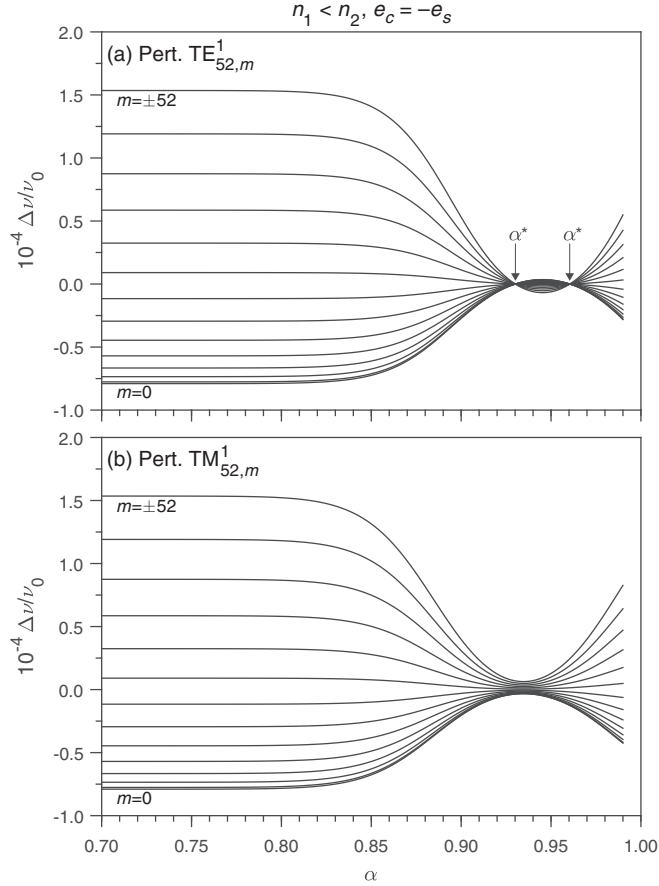


FIG. 9. Fractional shift of the (a) $\text{TE}_{52,m}^1$ and (b) $\text{TM}_{52,m}^1$ modes as a function of the core-shell ratio. The shell eccentricity is $e_s = 4.743 \times 10^{-4}$, with the core and shell eccentricities related by $e_c = -e_s$, and the shell (core) refractive index is $n_1 = 1.33$ ($n_2 = 1.41$).

$$C_{lm}^{\text{TM}(1)} = \int_0^\pi \sin \theta d\theta \left[|\mathbf{X}_{lm}|^2 [X_1^{33}(x_1^{(0)})]' x_1^{(1)} + P_l^m \frac{dP_l^m}{d\theta} \frac{dx_1^{(1)}}{d\theta} Y_1^{33}(x_1^{(0)}) \right], \quad (\text{A23})$$

$$D_{lm}^{\text{TM}(1)} = \int_0^\pi \sin \theta d\theta \left[|\mathbf{X}_{lm}|^2 [X_2^{11}(x_2^{(0)})]' x_2^{(1)} + P_l^m \frac{dP_l^m}{d\theta} \frac{dx_2^{(1)}}{d\theta} Y_2^{11}(x_2^{(0)}) \right]. \quad (\text{A24})$$

APPENDIX B: TERMS FOR TM MODES

Here we sketch how the formulas for A_l , B_l , and R_l^{TM} are obtained. We start by solving for $k^{(1)}$ by using Eqs. (A17)–

(A24), for which we get an equation of the form

$$\frac{k^{(1)}}{k^{(0)}} = \frac{-E}{a_1 E + a_2 F} \sum_L h_L^{(1)} \left[1 - \frac{E-G}{E} \frac{L(L+1)}{2l(l+1)} \right] \frac{\langle P_l^m | P_L | P_l^m \rangle}{\langle P_l^m | P_l^m \rangle} + \frac{-F}{a_1 E + a_2 F} \sum_L h_L^{(2)} \left[1 - \frac{F-H}{F} \frac{L(L+1)}{2l(l+1)} \right] \frac{\langle P_l^m | P_L | P_l^m \rangle}{\langle P_l^m | P_l^m \rangle}. \quad (\text{B1})$$

The terms E – H are defined as

$$E = X_2^{31} [X_1^{31}]' - X_2^{11} [X_1^{33}]', \quad (\text{B2})$$

$$F = X_1^{31} [X_2^{31}]' - X_1^{33} [X_2^{11}]', \quad (\text{B3})$$

$$G = X_2^{31} Y_1^{31} - X_2^{11} Y_1^{33}, \quad (\text{B4})$$

$$H = X_1^{31} Y_2^{31} - X_1^{33} Y_2^{11}. \quad (\text{B5})$$

Defining $R_l^{\text{TM}} = F/E$, we have that

$$R_l^{\text{TM}} = \frac{X_1^{31} [X_2^{31}]' - X_1^{33} [X_2^{11}]'}{X_2^{31} [X_1^{31}]' - X_2^{11} [X_1^{33}]'} = \left(\frac{X_1^{31}}{X_2^{11}} \right)^2 \frac{X_2^{11} [X_2^{31}]' - X_2^{31} [X_2^{11}]'}{X_1^{33} [X_1^{31}]' - X_1^{31} [X_1^{33}]'}, \quad (\text{B6})$$

where we used the resonance condition to get the last equality. Expanding all the terms and using the Wronskian recovers the expression in the main text. Now defining $B_l = (E - G)/E$, we have

$$B_l = \frac{X_2^{31} [X_1^{31}]' - X_2^{11} [X_1^{33}]' - [X_2^{31} Y_1^{31} - X_2^{11} Y_1^{33}]}{X_2^{31} [X_1^{31}]' - X_2^{11} [X_1^{33}]'} = \frac{X_2^{31} Z_1^{31} - X_2^{11} Z_1^{33}}{X_2^{31} [X_1^{31}]' - X_2^{11} [X_1^{33}]'}, \quad (\text{B7})$$

where Z_i^{jk} is defined so that $[X_i^{jk}]' = Y_i^{jk} + Z_i^{jk}$. Using the resonance condition and a bit of manipulation,

$$B_l = \frac{X_1^{33} Z_1^{31} - X_1^{31} Z_1^{33}}{X_1^{33} [X_1^{31}]' - X_1^{31} [X_1^{33}]'} = \frac{1}{1 + \frac{X_1^{33} Y_1^{31} - X_1^{31} Y_1^{33}}{X_1^{33} Z_1^{31} - X_1^{31} Z_1^{33}}}. \quad (\text{B8})$$

After expanding the denominator of the above expression and using the Wronskian, it is found that

$$\frac{X_1^{33} Y_1^{31} - X_1^{31} Y_1^{33}}{X_1^{33} Z_1^{31} - X_1^{31} Z_1^{33}} = \frac{l(l+1)}{(n_1 x_1)^2} \left(\frac{\xi_l(x_1)}{\xi_l'(x_1)} \right)^2. \quad (\text{B9})$$

This yields the term

$$B_l = \left[1 + \frac{l(l+1)}{(n_1 x_1)^2} \left(\frac{\xi_l(x_1)}{\xi_l'(x_1)} \right)^2 \right]^{-1}. \quad (\text{B10})$$

From the above, it is easy to see that $A_l = (F - H)/F$ is obtained by following the same steps.

[1] R. D. Richtmyer, Dielectric resonators, *J. Appl. Phys.* **10**, 391 (1939).

[2] K. J. Vahala, Optical microcavities, *Nature (London)* **424**, 839 (2003).

- [3] P. T. Kristensen and S. Hughes, Modes and mode volumes of leaky optical cavities and plasmonic nanoresonators, *ACS Photon.* **1**, 2 (2014).
- [4] P. T. Leung and K. M. Pang, Completeness and time-independent perturbation of morphology-dependent resonances in dielectric spheres, *J. Opt. Soc. Am. B* **13**, 805 (1996).
- [5] K. M. Lee, P. T. Leung, and K. M. Pang, Iterative perturbation scheme for morphology-dependent resonances in dielectric spheres, *J. Opt. Soc. Am. A* **15**, 1383 (1998).
- [6] P. T. Kristensen, C. Van Vlack, and S. Hughes, Generalized effective mode volume for leaky optical cavities, *Opt. Lett.* **37**, 1649 (2012).
- [7] N. Riesen, T. Reynolds, A. Francois, M. R. Henderson, and T. M. Monro, Q-factor limits for far-field detection of whispering gallery modes in active microspheres, *Opt. Express* **23**, 28896 (2015).
- [8] Y. Zhi, J. Valenta, and A. Meldrum, Structure of whispering gallery mode spectrum of microspheres coated with fluorescent silicon quantum dots, *J. Opt. Soc. Am. B* **30**, 3079 (2013).
- [9] M. L. Gorodetsky, A. A. Savchenkov, and V. S. Ilchenko, Ultimate Q of optical microsphere resonators, *Opt. Lett.* **21**, 453 (1996).
- [10] P. T. Kristensen, K. Herrmann, F. Intravaia, and K. Busch, Modeling electromagnetic resonators using quasinormal modes, *Adv. Opt. Photon.* **12**, 612 (2020).
- [11] F. Alpeggiani, N. Parappurath, E. Verhagen, and L. Kuipers, Quasinormal-Mode Expansion of the Scattering Matrix, *Phys. Rev. X* **7**, 021035 (2017).
- [12] P. Debye, Der lichtdruck auf kugeln von beliebigem material, *Ann. Phys. (Leipzig)* **335**, 57 (1909).
- [13] C. C. Lam, P. T. Leung, and K. Young, Explicit asymptotic formulas for the positions, widths, and strengths of resonances in Mie scattering, *J. Opt. Soc. Am. B* **9**, 1585 (1992).
- [14] M. B. Doost, W. Langbein, and E. A. Muljarov, Resonant-state expansion applied to three-dimensional open optical systems, *Phys. Rev. A* **90**, 013834 (2014).
- [15] K. M. Lee, P. T. Leung, and K. M. Pang, Dyadic formulation of morphology-dependent resonances. I. Completeness relation, *J. Opt. Soc. Am. B* **16**, 1409 (1999).
- [16] K. M. Lee, P. T. Leung, and K. M. Pang, Dyadic formulation of morphology-dependent resonances. II. Perturbation theory, *J. Opt. Soc. Am. B* **16**, 1418 (1999).
- [17] S. Ng, P. Leung, and K. Lee, Dyadic formulation of morphology-dependent resonances. III. Degenerate perturbation theory, *J. Opt. Soc. Am. B* **19**, 154 (2002).
- [18] R. Dubertrand, E. Bogomolny, N. Djellali, M. Lebental, and C. Schmit, Circular dielectric cavity and its deformations, *Phys. Rev. A* **77**, 013804 (2008).
- [19] J. Gohsrich, T. Shah, and A. Aiello, Perturbation theory of nearly spherical dielectric optical resonators, *Phys. Rev. A* **104**, 023516 (2021).
- [20] A. Aiello, J. G. E. Harris, and F. Marquardt, Perturbation theory of optical resonances of deformed dielectric spheres, *Phys. Rev. A* **100**, 023837 (2019).
- [21] W. Yan, P. Lalanne, and M. Qiu, Shape Deformation of Nanoresonator: A Quasinormal-Mode Perturbation Theory, *Phys. Rev. Lett.* **125**, 013901 (2020).
- [22] A. K. Ray and R. Nandakumar, Simultaneous determination of size and wavelength-dependent refractive indices of thin-layered droplets from optical resonances, *Appl. Opt.* **34**, 7759 (1995).
- [23] M. R. Foreman and F. Vollmer, Optical Tracking of Anomalous Diffusion Kinetics in Polymer Microspheres, *Phys. Rev. Lett.* **114**, 118001 (2015).
- [24] A. Moridnejad, T. C. Preston, and U. K. Krieger, Tracking water sorption in glassy aerosol particles using morphology-dependent resonances, *J. Phys. Chem. A* **121**, 8176 (2017).
- [25] D. L. Bones, J. P. Reid, D. M. Lienhard, and U. K. Krieger, Comparing the mechanism of water condensation and evaporation in glassy aerosol, *Proc. Natl. Acad. Sci. USA* **109**, 11613 (2012).
- [26] D. M. Lienhard, A. J. Huisman, D. L. Bones, Y.-F. Te, B. P. Luo, U. K. Krieger, and J. P. Reid, Retrieving the translational diffusion coefficient of water from experiments on single levitated aerosol droplets, *Phys. Chem. Chem. Phys.* **16**, 16677 (2014).
- [27] S. Bastelberger, U. K. Krieger, B. P. Luo, and T. Peter, Time evolution of steep diffusion fronts in highly viscous aerosol particles measured with Mie resonance spectroscopy, *J. Chem. Phys.* **149**, 244506 (2018).
- [28] D. J. Stewart, C. Cai, J. Nayler, T. C. Preston, J. P. Reid, U. K. Krieger, C. Marcolli, and Y. H. Zhang, Liquid-liquid phase separation in mixed organic/inorganic single aqueous aerosol droplets, *J. Phys. Chem. A* **119**, 4177 (2015).
- [29] K. Gorkowski, H. Beydoun, M. Aboff, J. S. Walker, J. P. Reid, and R. C. Sullivan, Advanced aerosol optical tweezers chamber design to facilitate phase-separation and equilibration timescale experiments on complex droplets, *Aerosol Sci. Technol.* **50**, 1327 (2016).
- [30] K. Gorkowski, N. M. Donahue, and R. C. Sullivan, Emulsified and liquid-liquid phase-separated states of α -pinene secondary organic aerosol determined using aerosol optical tweezers, *Environ. Sci. Technol.* **51**, 12154 (2017).
- [31] K. Gorkowski, N. M. Donahue, and R. C. Sullivan, Emerging investigator series: Determination of biphasic core-shell droplet properties using aerosol optical tweezers, *Environ. Sci.: Process. Imp.* **20**, 1512 (2018).
- [32] I. Teraoka and S. Arnold, Enhancing the sensitivity of a whispering-gallery mode microsphere sensor by a high-refractive-index surface layer, *J. Opt. Soc. Am. B* **23**, 1434 (2006).
- [33] D. Ristić, A. Chiappini, M. Mazzola, D. Farnesi, G. Nunzi Conti, G. C. Righini, P. Féron, G. Cibiel, M. Ferrari, and M. Ivanda, Whispering gallery mode profiles in a coated microsphere, *Eur. Phys. J.: Spec. Top.* **223**, 1959 (2014).
- [34] G. Chen, R. K. Chang, S. C. Hill, and P. W. Barber, Frequency splitting of degenerate spherical cavity modes: Stimulated Raman scattering spectrum of deformed droplets, *Opt. Lett.* **16**, 1269 (1991).
- [35] A. J. Trevitt, P. J. Wearne, E. J. Bieske, and M. D. Schuder, Observation of nondegenerate cavity modes for a distorted polystyrene microsphere, *Opt. Lett.* **31**, 2211 (2006).
- [36] S. C. Yorulmaz, M. Mestre, M. Muradoglu, B. E. Alaca, and A. Kiraz, Controlled observation of nondegenerate cavity modes in a microdroplet on a superhydrophobic surface, *Opt. Commun.* **282**, 3024 (2009).

- [37] A. Rafferty, K. Gorkowski, A. Zuend, and T. C. Preston, Optical deformation of single aerosol particles, *Proc. Natl. Acad. Sci. USA* **116**, 19880 (2019).
- [38] H. M. Lai, P. T. Leung, K. Young, P. W. Barber, and S. C. Hill, Time-independent perturbation for leaking electromagnetic modes in open systems with application to resonances in microdroplets, *Phys. Rev. A* **41**, 5187 (1990).
- [39] C. R. Ruehl, J. F. Davies, and K. R. Wilson, An interfacial mechanism for cloud droplet formation on organic aerosols, *Science* **351**, 1447 (2016).
- [40] J. Ovadnevaite, A. Zuend, A. Laaksonen, K. J. Sanchez, G. Roberts, D. Ceburnis, S. Decesari, M. Rinaldi, N. Hodas, M. C. Facchini, J. H. Seinfeld, and C. O'Dowd, Surface tension prevails over solute effect in organic-influenced cloud droplet activation, *Nature (London)* **546**, 637 (2017).
- [41] L. Kai and A. D'Alessio, Electromagnetic resonance at the interface of two concentric spheres, *J. Mod. Opt.* **42**, 1603 (1995).
- [42] B. Vennes and T. C. Preston, Calculating and fitting morphology-dependent resonances of a spherical particle with a concentric spherical shell, *J. Opt. Soc. Am. A* **36**, 2089 (2019).
- [43] W. Zheng and S. Ström, The null-field approach to electromagnetic resonance of composite objects, *Comput. Phys. Commun.* **68**, 157 (1991).
- [44] M. M. Sternheim and J. F. Walker, Non-Hermitian Hamiltonians, decay states, and perturbation theory, *Phys. Rev. C* **6**, 114 (1972).
- [45] P. Barber and C. Yeh, Scattering of electromagnetic waves by arbitrarily shaped dielectric bodies, *Appl. Opt.* **14**, 2864 (1975).
- [46] D.-S. Wang and P. Barber, Scattering by inhomogeneous non-spherical objects, *Appl. Opt.* **18**, 1190 (1979).
- [47] M. I. Mishchenko, L. D. Travis, and A. A. Lacis, *Scattering, Absorption, and Emission of Light by Small Particles* (Cambridge University Press, Cambridge, 2002).
- [48] J. F. Owen, R. K. Chang, and P. W. Barber, Morphology-dependent resonances in Raman scattering, fluorescence emission, and elastic scattering from microparticles, *Aerosol Sci. Technol.* **1**, 293 (1982).